Desalination 570 (2024) 117081

Contents lists available at ScienceDirect

Desalination

journal homepage: www.elsevier.com/locate/desal

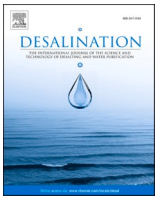

Innovative system for BWRO desalination powered by PV and pumped hydro storage – Economic and GHG emissions analysis

Anas Sanna [a,b,*], Wolfgang Streicher [b]

[a] Institute of Environmental Technology and Energy Economics (IUE), Hamburg University of Technology (TUHH), Eissendorfer Str. 40, 21073 Hamburg, Germany
[b] Unit of Energy Efficient Buildings, Department of Structural Engineering and Material Sciences, University of Innsbruck, Techniker Str. 13, A-6020 Innsbruck, Austria

HIGHLIGHTS

- Innovative system for BWRO plant driven by PV system and pumped hydro storage.
- Economic assessment and GHG emissions analysis of the innovative system.
- Comparison with the state of the art and conventional BWRO systems.
- For off-grid operation, the innovative system is the most economical system.
- For off-grid operation, the innovative system produces the lowest GHG emissions.

ARTICLE INFO

Keywords:
Drinking water
Reverse osmosis desalination
Photovoltaic
Pumped hydro storage
Economic analysis
GHG emissions analysis

ABSTRACT

Brackish water reverse osmosis (BWRO) desalination driven by photovoltaic (PV) system as a primary energy source and pumped hydro storage (PHS) as an intermediate storage offers an energy-efficient and competitive solution to overcome freshwater scarcity. This innovative system for drinking water production from brackish groundwater was developed and technically analyzed in a prior work. In this paper, the entire system with two power supply scenarios: scenario 1 (PV, PHS and battery storage) and scenario 2 (PV, PHS and grid) is economically assessed and its greenhouse gas (GHG) emissions are analyzed. Thereafter, this system is compared with the state-of-the-art and BWRO systems powered by a conventional energy source (grid or diesel generator) to discuss and evaluate the future role of this innovative system in the BWRO desalination market. For off-grid operation, the innovative system with scenario 1 is the most economical system for drinking water production from brackish groundwater compared to the other examined systems as long as the diesel fuel price is equal to or more expensive than 0.58 US$/L. Moreover, the minimum specific GHG emissions produced per unit of drinking water production in scenario 1 is 46.8 % less than in the current system (PV and battery storage).

1. Introduction

Desalination of brackish water (BW) and seawater (SW) has become one of the most crucial solutions worldwide for the provision of drinking water (DW) in areas with inadequate freshwater resources [1,2]. Currently, about 16,000 desalination plants are operational in 177 countries with a total production capacity of roughly 95.4 million m^3/d (34.8 billion m^3/year) [3,4]. Thus, these desalination plants produce the daily needs of more than 300 million people around the world [5]. The challenge for desalination of BW and SW is that the desalination processes typically require a high energy demand compared to conventional water treatment processes [6]. The energy required by the desalination plants is mainly generated from fossil fuels [7,8]. However, the burning of fossil fuels produces significant amounts of greenhouse gas (GHG) emissions associated with negative environmental impacts [9]. The heavy dependence on limited fossil fuel resources also ties the costs of DW production from BW and SW to variable prices of fossil fuel. Furthermore, the use of fossil fuels is characterized by supply uncertainties, especially in crisis situations [10]. Therefore, in recent years, renewable energy sources were used as an alternative to fossil fuels for the generation of the energy required for desalination applications [3,11].

Water desalination plants powered by renewable energies are

* Corresponding author at: Institute of Environmental Technology and Energy Economics (IUE), Hamburg University of Technology (TUHH), Eissendorfer Str. 40, 21073 Hamburg, Germany.
E-mail address: a.sanna@tuhh.de (A. Sanna).

https://doi.org/10.1016/j.desal.2023.117081
Received 27 June 2023; Received in revised form 24 September 2023; Accepted 17 October 2023
Available online 25 October 2023

attractive, sustainable, and environmentally friendly solutions for providing DW where salt water (BW or SW) is available [12–15]. Water desalination plants can be operated with solar, wind, geothermal, biomass, wave, and/or tidal energy, depending on the desalination technology as well as locally available renewable energy sources [16]. Commercial water desalination technologies are categorized into two main process groups: thermal processes (mainly multiple effect distillation and multi-stage flash distillation) and membrane processes (mainly reverse osmosis (RO) and electrodialysis) [17]. Nowadays, RO is the most widely utilized desalination technology in the world as it is the most economical technology for freshwater production from BW and SW [18]. Moreover, RO technology is the most energy-efficient desalination technology [19] and thus has the lowest GHG emissions during the operation phase [7].

RO desalination plants require as energy primarily only electricity to operate the pumps of the whole plant [10]. The electricity consumption for DW production by BWRO desalination plants is typically one to four times less than by SWRO desalination plants [20]. Furthermore, solar irradiation is very high (up to 2750 kWh/m^2 per year) in zones where the freshwater scarcity problem is very severe and rapidly increasing [21,22]. Therefore, BWRO plants powered by photovoltaic (PV) systems are interesting solutions to overcome freshwater scarcity worldwide [10].

The current systems for BWRO desalination based on PV are mostly either connected to the national power grid or include an electricity storage system in order to ensure a stable and continuous power supply [23–25]. In the grid connection case, these systems may overload the national power grid, especially in areas with underdeveloped electricity supply infrastructure, at night and on cloudy days, since the total electric power required by the whole BWRO plant is drawn from the national power grid. In the off-grid case, battery storage (BS) systems are the most widespread electricity storage technologies, since BS systems are characterized by a comparatively high efficiency [3]. However, at least 5 % of the electric energy to be stored is lost during charging and discharging the BS system [26]. Moreover, the BS systems have some drawbacks, such as environmental hazards due to its content of heavy metals, low energy density and comparatively high specific cost [27,28].

For the above reasons, an innovative system for a BWRO plant based on PV system as the main energy source and pumped hydro storage (PHS) system as intermediate storage was developed the year before last. The PS system is used to cover the hydraulic energy required by the BWRO desalination process when the required power for the BWRO desalination process cannot be provided by the PV system. The total energy efficiency of this PHS system is 2.4 % higher than the total energy efficiency for a BS system in the current designs for a BWRO plant powered by PV system and BS system [29]. This novel system was technically analyzed in [29] and investigated with two scenarios for power supply (off-grid and with grid connection). In the off-grid scenario, a BS system with a very low electric storage capacity was also needed. The BS system or the national power grid was only used to cover the electric power required by the pumps with low electric power consumption and by the disinfection processes if adequate electric power cannot be generated by the PV system [29]. Therefore, this innovative system contributes to avoid an overload of the national power grid even in the case with the grid connection.

In this paper, the innovative system for a BWRO plant powered by PV system and PHS system is economically assessed, and its GHG emissions are determined and analyzed. This system is also compared with the state-of-the-art and the conventional BWRO systems for DW production in order to discuss and evaluate the future role of this innovative system in the BWRO desalination market. The comparison with the current and conventional BWRO systems for DW production is performed under the same framework conditions, such as BW composition, well depth, solar irradiation, and configuration of the BWRO plant. Therefore, the innovative system with the two power supply scenarios: off-grid scenario (scenario 1: PV, PHS and BS) and grid-connected scenario (scenario 2: PV, PHS and grid), two current systems as the state-of-the-art: off-grid design (system A: PV and BS) and grid-connected design (system B: PV and grid), as well as two conventional systems: off-grid design (system C: diesel generator) and grid-connected design (System D: grid) are modelled and investigated at the same reference site. Fig. 1 illustrates the energy resources and storage systems of the examined systems.

The operation of the examined systems is simulated on an hourly basis for a whole year. Thus, the required nominal output of the energy resources as well as the necessary storage capacity of the used storage systems is identified. Since the required storage capacity of the storage system depends on the installed nominal output of the PV system, the costs and the GHG emissions for DW production by the innovative and current systems are calculated as a function of the installed nominal output of the PV system. Thereby, the minimum costs and GHG emissions for DW production by these systems are determined. The costs for DW production by the conventional systems are calculated in dependence of the price of diesel fuel and electricity. Thereafter, it is determined at what price of diesel fuel and electricity the innovative and current systems become more economical than the conventional systems. Moreover, a sensitivity analysis is conducted for all examined systems in order to discuss and evaluate the impact of changes in the input parameters used for the economic and GHG emissions analysis on the simulation results.

2. Methodology

In order to economically analyze the examined systems for DW production from brackish groundwater (BGW) and to determine their GHG emissions, the examined systems are first technically modelled under the same framework conditions. The methodological approaches for the technical modeling, as well as for the economic and GHG emissions analysis for the examined systems are presented below.

2.1. Technical modeling

The following shows how the below mentioned systems, for DW production from BGW, are simulated.

- An innovative system with two power supply scenarios: scenario 1 (PV, PHS and BS), and scenario 2 (PV, PHS and grid),
- Two current systems as the state-of-the-art: system A (PV and BS), and system B (PV and grid), and
- Two conventional systems: system C (diesel generator), and system D (grid)

In the innovative system with scenarios 1 and 2 and in the two current systems (system A and system B), the PV system should cover the annual electricity demand of the entire system for DW production from BGW. Over the course of the year, the total amount of electricity that the BWRO plant draws from the national power grid in scenario 2 and system B is fed back from the PV system into the national power grid when the generated PV electric power cannot be used for the system. The annual amount of electricity fed into the national power grid from the PV system ($W_{feed\text{-}in}$) should be equal to or greater than the annual amount of electricity that the BWRO plant draws from the national power grid (W_{pg}).

In all examined systems, the BWRO plant is continuously (24 h/d) operated with a constant DW production capacity (Q_{DW}). The BWRO plant includes three treatment processes: BW pre-treatment, BWRO desalination, and permeate post-treatment. In the BWRO desalination process, a part of the brine flow is returned back into the feed flow by a booster pump to increase the water recovery of the BWRO desalination process. For disposal of the surplus brine, evaporation ponds consisting of shallow basins are used. Evaporation ponds are one of the most applied methods for evaporating the reject brine from inland BWRO plants using solar radiation in highly dry regions [30,31]. The individual

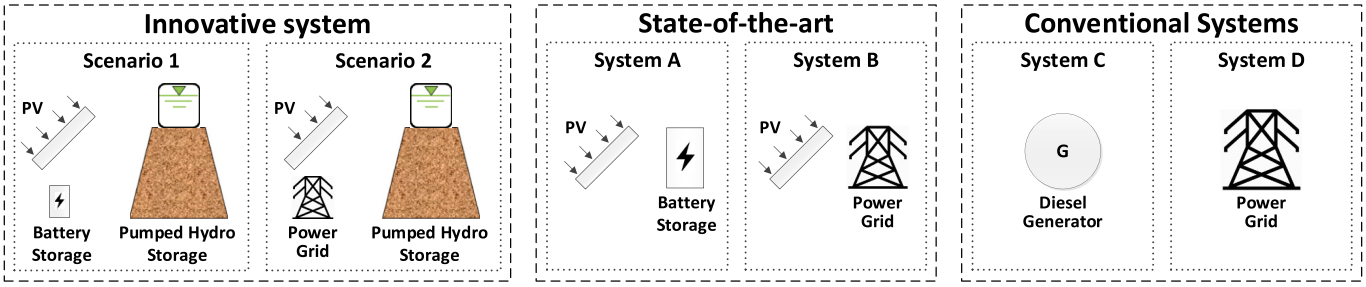

Fig. 1. Energy resources and storage systems in the innovative system with two power supply scenarios (scenario 1 and scenario 2), as well as in two current systems (state-of-the-art) and two conventional systems for drinking water production from brackish groundwater.

components of the examined systems (BWRO plant, evaporation ponds, PV system, PHS system, and BS system) are modelled using the same method as detailed in [29]. Thereafter, the operation of the examined systems is simulated on an hourly basis for a whole year in MATLAB-Simulink [32].

2.1.1. Innovative system

The operation of the entire system is modelled in two power supply scenarios: off-grid scenario (scenario 1: PV, PHS and BS) and grid-connected scenario (scenario 2: PV, PHS and grid). In scenario 1, the electricity for running the entire innovative system (BWRO plant and energy storage (ES) system) comes only from the PV system. The ES system includes a PHS system as an intermediate storage device, as well as a BS system as an electric ES device. In scenario 2, the ES system consists only of the PHS system. Instead of using the BS system, the innovative system is connected to the national power grid (Fig. 2) [29].

In this work, the PHS system consists of two major components: a high-pressure pump and an elevated reservoir situated on a mountain. The PHS system in both scenarios is used to cover the hydraulic energy required by the BWRO desalination process partially or even completely when the electric power produced by the PV system (EP_{PV}) is lower than the electric power consumption of the whole BWRO plant (EP_{BWRO}). The BS system in scenario 1 or the national power grid in scenario 2 is used to cover the electric power consumption of the brine recirculation pump, the post-treatment process, and the disinfection of the BW stored in the elevated reservoir (EP_{BPPo}) when the EP_{PV} is lower than the EP_{BPPo} [29]. The following briefly describes only the main operating rules for the entire system, depending on EP_{PV}.

- If $EP_{PV} \geq EP_{BWRO}$, the whole BWRO plant is powered only by PV electric power. The surplus electric power produced by the PV system is used to charge the PHS system (in scenarios 1 and 2) and the BS system (in scenario 1) or fed into the national power grid (in scenario 2).
- If $EP_{BWRO} > EP_{PV} \geq EP_{BPPo}$, the BWRO plant is powered by PV electric power and hydraulic power from the PHS system (in scenarios 1 and 2). The stored BGW is fed back from the PHS system into the BWRO desalination process as feed flow.
- If $EP_{BPPo} > EP_{PV} > 0$, the BWRO plant is powered by hydraulic power from the PHS system and electric power from the PV System (in

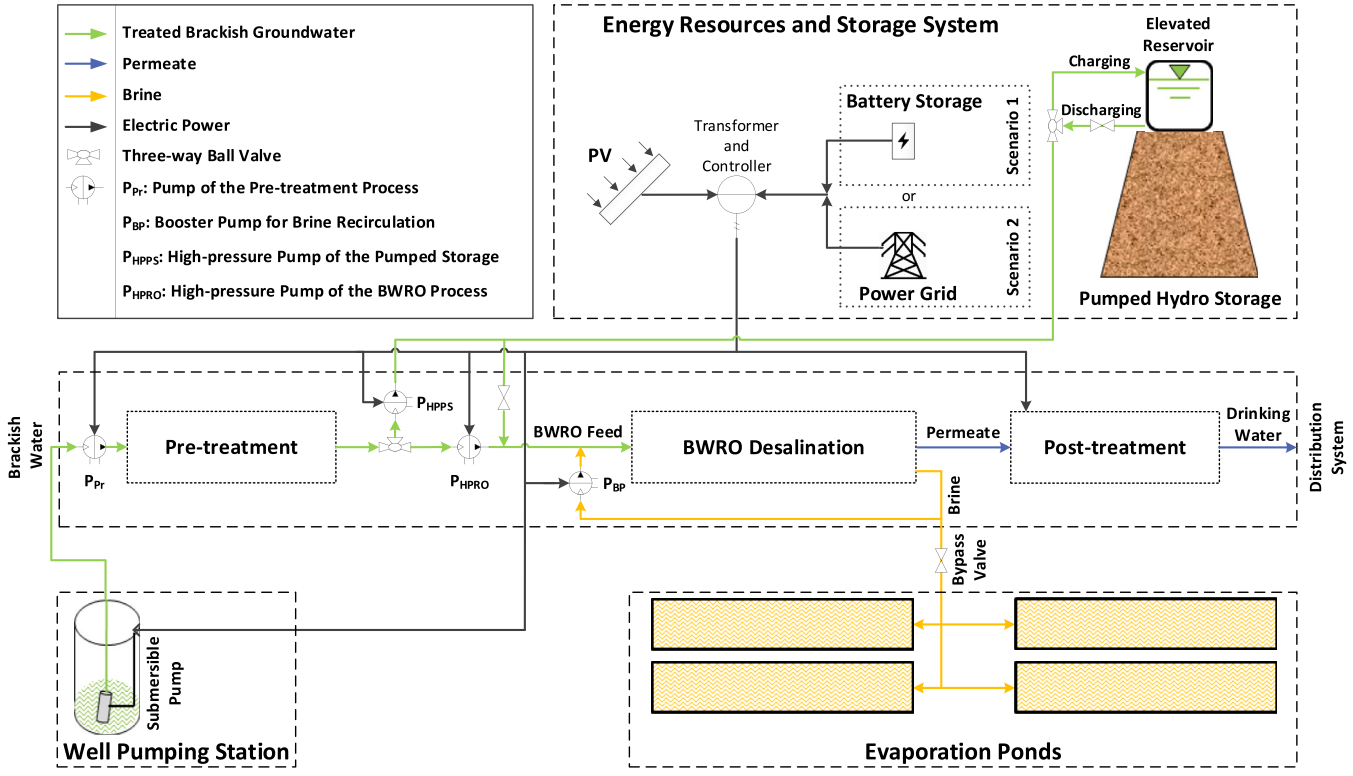

Fig. 2. Innovative system for drinking water production from brackish groundwater. The system can be operated with two power supply scenarios: scenario 1 (PV, PHS and BS) or scenario 2 (PV, PHS and grid) [29].

scenarios 1 and 2), as well as by electric power from the BS System (in scenario 1) or from the national power grid (in scenario 2).
- If $EP_{PV} = 0$, the BWRO plant is powered by hydraulic power from the PHS system (in scenarios 1 and 2), as well as by electric power from the BS System (in scenario 1) or from the national power grid (in scenario 2) [29].

Both power supply scenarios are simulated as detailed in [29]. Thus, the minimum required nominal output of the PV system is first determined. Thereafter, the installed nominal output of the PV system ($P_{n\text{-}PV}$) is increased to decrease the required storage capacity of the PHS system ($V_{ER\text{-}max}$) as well as the BS system ($BS_{c\text{-}max}$) and thereby to optimize (minimize) the specific unit cost of DW production (UPC_{DW}) (Section 2.2) and the specific GHG emissions produced per unit of DW production (SE_{UPW}) (Section 2.3).

2.1.2. State-of-the-art

Two current systems for BWRO desalination powered by PV with (BS system or power grid) are simulated [3,25,33].

2.1.2.1. System A: PV and BS. It is an off-grid design including a PV system as a main energy source, and a BS system as an electric ES device (Fig. A.1 in Appendix A). The BS system is designed to cover the EP_{BWRO} when the EP_{PV} is lower than the EP_{BWRO} [3,29,34]. If the EP_{PV} exceeds the EP_{BWRO}, the whole BWRO plant is powered only by PV electric power. The surplus electric power produced by the PV system is used for charging the BS system.

The operation of the entire system is simulated as detailed in [29]. Thus, the minimum required nominal output of the PV system is first determined. Thereafter, the $P_{n\text{-}PV}$ is increased to reduce the $BS_{c\text{-max}}$ and thereby to optimize (minimize) the UPC_{DW} (Section 2.2) and the SE_{UPW} (Section 2.3).

2.1.2.2. System B: PV and grid. The system is connected to the national power grid (Fig. A.1 in Appendix A) [12]. However, if the EP_{PV} exceeds the EP_{BWRO}, the whole BWRO plant is powered only by the electricity produced by the PV system. The surplus electric power from the PV system is fed into the national power grid (Eq. (1)).

$$EP_{feed-in} = EP_{PV} - EP_{BWRO} \tag{1}$$

$EP_{feed\text{-}in}$ is the feed-in electric power. The BWRO plant draws electricity from the national power grid when the EP_{PV} is lower than the EP_{BWRO} (Eq. (2)) [29].

$$EP_{pg} = EP_{BWRO} - EP_{PV} \tag{2}$$

EP_{pg} is the electric power consumption from the national power grid. Based on the key criteria for the system operation outlined above, the minimum required nominal output of the PV system is determined.

2.1.3. Conventional systems

Two systems for BWRO desalination powered completely (100 %) by a conventional energy source (diesel generator or power grid) are simulated. Therefore, no PV system is used for these two conventional systems.

2.1.3.1. System C: diesel generator. In system C, the EP_{BWRO} is provided by a diesel generator. Therefore, the rated output of the required diesel generator ($P_{r\text{-}DG}$) should be equal to or greater than the EP_{BWRO}. The hourly fuel consumption of the diesel generator (F_{DG}) is calculated by using the following equation [35].

$$F_{DG} = f_s\, EP_{DG} + f_i\, P_{r-DG} \tag{3}$$

EP_{DG} is the electric power produced by the diesel generator. f_s and f_i are the slope coefficient and the intercept coefficient for the generator fuel curve.

2.1.3.2. System D: grid. In system D, the BWRO plant is connected to the national power grid. The EP_{BWRO} is supplied by the national power grid 24 h/d [12]. Therefore, in this case, the EP_{pg} is exactly equal to the EP_{BWRO}.

2.2. Economic analysis

In order to make the investigated innovative system with scenarios 1 and 2, as well as the current and conventional systems comparable with each other with regard to their economic efficiency, the UPC_{DW} is determined for all examined cases. The UPC_{DW} is calculated based on the capital expenditure and the operating expenditure of the entire system ($CAPEX_{sys}$ and $OPEX_{sys}$) using the annuity method [12,36] (Eq. (4)).

$$UPC_{DW} = \frac{1}{\sum_{t=1}^{8760} Q_{DW}\, t_{BWRO}} \left(CAPEX_{sys}\, \frac{Ir\,(1+Ir)^n}{(1+Ir)^n - 1} + OPEX_{sys} \right) \tag{4}$$

Ir is the interest rate, n is the economic project lifetime, and t_{BWRO} is the operating time of the BWRO plant. The $CAPEX_{sys}$ includes all costs related to the procurement and construction of the project (BWRO plant, evaporation ponds, energy resources, and ES system) as well as engineering and other costs. The $OPEX_{sys}$ reflective all costs for diesel fuel consumption and/or operation and maintenance of system equipment as well as replacement of consumables over the course of the year [37,38]. However, if the system is connected to the national power grid, the annual cost of the share of the PV electricity that is fed into the national power grid and exceeds the total electricity consumption for the whole BWRO plant from the national power grid ($\Delta EC_{feed\text{-}in}$) (Section 2.2.4) must be subtracted from the $OPEX_{sys}$ in order to determine the UPC_{DW}. Therefore, the UPC_{DW} in scenario 2 and system B is calculated by Eq. (5).

$$UPC_{DW} = \frac{1}{\sum_{t=1}^{8760} Q_{DW}\, t_{BWRO}} \left(CAPEX_{sys}\, \frac{Ir\,(1+Ir)^n}{(1+Ir)^n - 1} + OPEX_{sys} - \Delta EC_{feed-in} \right) \tag{5}$$

The following describes how the capital expenditure ($CAPEX$) and the operating expenditure ($OPEX$) of the individual components of the examined systems for DW production from BGW are determined.

2.2.1. BWRO plant

The $CAPEX$ of the whole BWRO plant ($CAPEX_{BWRO}$) is determined based on the Q_{DW} and the specific capital cost of the whole BWRO plant (SC_{BWRO}) (Eq. (6)) [39].

$$CAPEX_{BWRO} = 24\, Q_{DW}\, SC_{BWRO} \tag{6}$$

The total annual $OPEX$ of the whole BWRO plant ($OPEX_{BWRO}$) is the sum of the replacement cost of the BWRO membranes ($C_{r\text{-}m}$), the insurance cost (C_{ins}), the labor cost (C_{lab}), the chemical cost (C_{ch}), and the maintenance cost (C_{main}) (Eq. (7)) [36,40]. The costs of the required energy sources and storage for the operation of the BWRO plant are calculated separately in Sections 2.2.3, 2.2.4, 2.2.5, and 2.2.6.

$$OPEX_{BWRO} = C_{r-m} + C_{ins} + C_{lab} + C_{ch} + C_{main} \tag{7}$$

The following equations describe how $C_{r\text{-}m}$, C_{ins}, C_{lab}, C_{ch}, and C_{main} are calculated [36,40–42].

$$C_{r-m} = 0.2\, C_m \tag{8}$$

$$C_{ins} = 0.005\, CAPEX_{BWRO} \tag{9}$$

$$C_{lab} = 0.01 \sum_{t=1}^{8760} Q_{DW}\, t_{BWRO} \tag{10}$$

$$C_{ch} = 0.0225 \sum_{t=1}^{8760} Q_{Feed}\, t_{BWRO} \tag{11}$$

$$C_{main} = 0.01 \sum_{t=1}^{8760} Q_{DW}\, t_{BWRO} \tag{12}$$

C_m is the total capital cost of the BWRO membranes, and Q_{Feed} is the

flow rate of the feed water to the BWRO membranes.

2.2.2. Evaporation ponds

The *CAPEX* of the evaporation ponds ($CAPEX_{EP}$) is expressed as a function of the brine flow rate from the BWRO desalination process into the evaporation ponds ($Q_{B\text{-}EP}$) and the specific capital cost of the evaporation ponds (SC_{EP}) using Eq. (13). The SC_{EP} depends mainly on evaporation rate (local climate), the land and earthwork costs, and the liner costs [30,38,43].

$$CAPEX_{EP} = 24\ Q_{B-EP}\ SC_{EP} \tag{13}$$

The total annual *OPEX* of the evaporation ponds ($OPEX_{EP}$) is calculated by Eq. (14).

$$OPEX_{EP} = 0.01 \sum_{t=1}^{8760} Q_{B-EP}\ t_{BWRO} \tag{14}$$

2.2.3. PV system

In this paper, the cost calculation of the PV system also includes the cost of the inverter. The *CAPEX* of the PV system ($CAPEX_{PV}$) is calculated by Eq. (15) [39,44,45].

$$CAPEX_{PV} = (SC_{PV-m} + SC_{PV-i} + SC_{PV-si})\ P_{n-PV} \tag{15}$$

$SC_{PV\text{-}m}$, $SC_{PV\text{-}i}$, and $SC_{PV\text{-}si}$ are the specific costs of the PV modules, the inverter, and the substructure as well as installation (including power cables and controller units), respectively. The total annual *OPEX* of the PV system ($OPEX_{PV}$) is the sum of the annual costs for the operation and maintenance of the PV system (OM_{PV}), and the annual replacement cost of the inverter ($C_{r\text{-}PV\text{-}i}$) [44,46] (Eq. (16)).

$$OPEX_{PV} = OM_{PV} + C_{r-PV-i} = 0.02\ CAPEX_{PV} + \frac{No_{PV-i}}{n}\ C_{PV-i} \tag{16}$$

$C_{PV\text{-}i}$ is the capital cost of the inverter, and $No_{PV\text{-}i}$ is number of the inverters to be replaced over lifetime of the project. The levelized cost of electricity from the PV system ($LCOE_{PV}$) is determined based on the $CAPEX_{PV}$ and the $OPEX_{PV}$ using the annuity method [47–49] (Eq. (17)).

$$LCOE_{PV} = \frac{1}{\sum_{t=1}^{8760} EP_{PV}\ t_{PV}} \left(CAPEX_{PV}\ \frac{Ir\ (1+Ir)^n}{(1+Ir)^n - 1} + OPEX_{PV} \right) \tag{17}$$

t_{PV} is the operating time of the PV system.

2.2.4. Power grid

In the innovative system with scenario 2 (PV, PHS and grid) and in system B (PV and grid), the PV system is designed at the reference site to cover mainly the total electricity consumption for the operation of the whole BWRO plant (24 h/d over the year). Therefore, the net metering scheme is applied [50,51]. Over the course of the year, the W_{pg} is compensated by the electricity that the PV system feeds into the national power grid. If the $W_{feed\text{-}in}$ is higher than the W_{pg} at the end of the year, the $\Delta EC_{feed\text{-}in}$ is calculated by using Eq. (18).

$$\Delta EC_{feed-in} = \left(\sum_{t=1}^{8760} EP_{feed-in}\ t_{feed-in} - \sum_{t=1}^{8760} EP_{pg}\ t_{pg} \right) ST_{PV-surplus} \tag{18}$$

$t_{feed\text{-}in}$ is the feed-in time of electricity into the national power grid, t_{pg} is the time of electricity consumption from the national power grid, and $ST_{PV\text{-}surplus}$ is the specific tariff for purchasing surplus PV electricity by the distribution company.

In system D (grid), the annual cost of electricity that the BWRO plant draws from the national power grid (EC_{pg}) is determined by Eq. (19).

$$EC_{pg} = \sum_{t=1}^{8760} PE_{pg}\ EP_{pg}\ t_{pg} \tag{19}$$

PE_{pg} is the price of electricity from the national power grid.

2.2.5. Diesel generator

The *CAPEX* of the diesel generator ($CAPEX_{DG}$) is determined based on the $P_{r\text{-}DG}$ and the specific capital cost of the diesel generator (SC_{DG}) (Eq. (20)) [52].

$$CAPEX_{DG} = SC_{DG}\ P_{r-DG} \tag{20}$$

The total annual *OPEX* of the diesel generator ($OPEX_{DG}$) is calculated by Eq. (21) [46,53–55].

$$OPEX_{DG} = OM_{DG} + C_{DF} + C_{r-DG} \tag{21}$$

OM_{DG} is the annual cost for the operation and maintenance of the diesel generator, C_{DF} is the annual cost of diesel fuel, and $C_{r\text{-}DG}$ is the annual replacement cost of the diesel generator. The OM_{DG} is given by Eq. (22).

$$OM_{DG} = \sum_{t=1}^{8760} EP_{DG}\ t_{DG}\ SC_{OM-DG} \tag{22}$$

t_{DG} is the operating time of the diesel generator, and $SC_{OM\text{-}DG}$ are the specific costs for the operation and maintenance of the diesel generator. The C_{DF} is given by Eq. (23) [53,56].

$$C_{DF} = \sum_{t=1}^{8760} P_{DF}\ F_{DG}\ t_{DG} \tag{23}$$

P_{DF} is the diesel fuel price. The $C_{r\text{-}DG}$ is calculated by Eq. (24).

$$C_{r-DG} = \frac{\sum_{t=1}^{8760} t_{DG}}{N_{DG}}\ P_{r-DG}\ SC_{r-DG} \tag{24}$$

N_{DG} is the lifetime of the diesel generator and $SC_{r\text{-}DG}$ are specific costs for replacement of the diesel generator.

2.2.6. ES system

2.2.6.1. PHS system. The *CAPEX* of the PHS system ($CAPEX_{PHS}$) comprises the capital costs of the high-pressure pump of the PHS system (C_{HPPHS}), the water pipeline between the BWRO plant and the elevated reservoir (C_{Pi}), and the elevated reservoir (C_{ER}), as well as the costs for the electrical equipment, the controller units, and the installation (C_{eci}) (Eq. (25)) [44,57]. The C_{HPPHS}, C_{Pi}, C_{ER}, and C_{eci} are determined by Eq. (26), (27), (28), and (29), respectively [12,44,58,59].

$$CAPEX_{PHS} = C_{HPPHS} + C_{Pi} + C_{ER} + C_{eci} \tag{25}$$

$$C_{HPPHS} = 52\ (P_{HPPHS-max}\ \ Q_{HPPHS-max}) \tag{26}$$

$$C_{Pi} = L_{Pi}\ SC_{Pi} \tag{27}$$

$$C_{ER} = V_{ER-max}\ SC_{ER} \tag{28}$$

$$C_{eci} = 0.2\ (C_{HPPHS} + C_{Pi} + C_{ER}) \tag{29}$$

$P_{HPPHS\text{-}max}$, and $Q_{HPPHS\text{-}max}$ are the maximum operating pressure and the maximum operating flow rate of the high-pressure pump of the PHS system, L_{Pi} is the total length of the water pipeline between the BWRO plant and the elevated reservoir, SC_{Pi} is the specific capital cost of the water pipeline between the BWRO plant and the elevated reservoir, and SC_{ER} is the specific capital cost of the elevated reservoir. For small PHS systems, as in this work, the total annual *OPEX* of the PHS system ($OPEX_{PHS}$) can be calculated using Eq. (30) [60,61]. However, the $OPEX_{PHS}$ does not include the cost for the electricity consumption of the high-pressure pump of the PHS system, since the PHS system is powered only by the PV system.

$$OPEX_{PHS} = 0.03\ CAPEX_{PHS} \tag{30}$$

2.2.6.2. BS system. The *CAPEX* of the BS system ($CAPEX_{BS}$) is determined based on the maximum electric storage capacity of the BS system ($BS_{c\text{-max}}$), as well as the specific capital costs for the storage battery (SC_B) and the inverter with control units ($SC_{BS\text{-}con}$) (Eq. (31)).

$$CAPEX_{BS} = (SC_B + SC_{BS-con})\ BS_{c-max} \tag{31}$$

The total annual *OPEX* of the BS system ($OPEX_{BS}$) includes the annual costs for the operation and maintenance of the BS system (OM_{BS}) and the replacement cost of the storage battery ($C_{r\text{-}B}$) (Eq. (32)) [62]. Since the BS system is charged only with the electricity from the PV system, the $OPEX_{BS}$ does not include the cost of electricity for charging the BS system.

$$OPEX_{BS} = OM_{BS} + C_{r-B} = 0.014\ CAPEX_{BS} + \frac{No_B}{n}\ C_B \tag{32}$$

No_B is number of the storage batteries to be replaced over lifetime of the project, and C_B is the capital cost of the storage battery.

2.3. GHG emissions analysis

For all cases studied, the total annual amount of GHG emissions from the entire system (TE_{sys}), and the SE_{UPW} are determined. The SE_{UPW} are calculated in scenario 1, system A, system C and system D by using Eq. (33).

$$SE_{UPW} = \frac{TE_{sys}}{\sum_{t=1}^{8760} Q_{DW}\ t_{BWRO}} \tag{33}$$

The TE_{sys} includes the annual GHG emissions from all system components for each investigated case. If the system is connected to the national power grid, the annual amount of GHG emissions caused by the share of the PV electricity that is fed into the national power grid and exceeds the total electricity consumption for the whole BWRO plant from the national power grid ($\Delta E_{feed\text{-}in}$) must be subtracted from the TE_{sys} in order to determine the SE_{UPW}. Therefore, the SE_{UPW} in scenario 2 and system B are defined according to Eq. (34).

$$SE_{UPW} = \frac{TE_{sys} - \Delta E_{feed-in}}{\sum_{t=1}^{8760} Q_{DW}\ t_{BWRO}} \tag{34}$$

The following describes how the annual amount of GHG emissions from the individual components of the examined systems for DW production from BGW is determined.

2.3.1. BWRO plant

The power supply system for the BWRO plant is primarily responsible for most of the GHG emissions from the entire system for DW production from BW [63–66]. Therefore, the GHG emissions from the BWRO plant are not simulated at the component level. However, the total annual amount of GHG emissions from the whole BWRO plant (E_{BWRO}) is estimated based on the total annual amount of GHG emissions from the use of a conventional energy system to cover the total electric energy demand of the whole BWRO plant as described in Section 3.1.1.

2.3.2. Evaporation ponds

Brine disposal using the evaporation ponds is a natural process in which the water is evaporated from the reject brine by solar radiation [18,67]. In addition, the evaporation ponds require very low maintenance [68]. Therefore, no special GHG emissions from the evaporation ponds are considered, as in the current studies [7,30,63].

2.3.3. PV system

Electricity generation from the PV system is associated with GHG emissions caused primarily during manufacturing of materials for the PV system (which include PV modules, inverter, wiring, and the assembly structure), but also from the assembly and operation of the PV system [69,70]. The total annual amount of GHG emissions from the use of the PV system for electricity generation (E_{PV}) is determined by Eq. (35) [71].

$$E_{PV} = \sum_{t=1}^{8760} EP_{PV}\ t_{PV}\ SE_{PV} \tag{35}$$

SE_{PV} is the specific GHG emissions for electricity generation from the PV system.

2.3.4. Power grid

The GHG emissions due to electricity consumption from the national power grid depend on the production, transmission and distribution processes of electricity. In system D, the total annual amount of GHG emissions caused by the BWRO plant's electricity consumption from the national power grid (E_{pg}) is calculated by Eq. (36) [72,73].

$$E_{pg} = \frac{\sum_{t=1}^{8760} EP_{pg}\ t_{pg}\ SE_{pg}}{(1 - LF_{TD})} \tag{36}$$

SE_{pg} is the specific GHG emissions related to the electricity generation for the national power grid, and LF_{TD} is the factor for transmission and distribution losses.

In scenario 2 and system B, the $\Delta E_{feed\text{-}in}$ can be calculated by using Eq. (37).

$$\Delta E_{feed-in} = \left(\sum_{t=1}^{8760} EP_{feed-in}\ t_{feed-in} - \sum_{t=1}^{8760} EP_{pg}\ t_{pg} \right) SE_{PV} \tag{37}$$

2.3.5. Diesel generator

The annual amount of GHG emissions caused by the use of the diesel generator (E_{DG}) is calculated by Eq. (38) [71,74,75].

$$E_{DG} = \sum_{t=1}^{8760} F_{DG}\ t_{DG}\ EF_{DG} \tag{38}$$

EF_{DG} is the emission factor for the diesel fuel burned with the diesel generator.

2.3.6. ES system

2.3.6.1. PHS system. The temporary storing of hydraulic energy using the PHS system is associated with GHG emissions, which are mainly caused during the construction of the PHS system. The total annual amount of GHG emissions from the use of the PHS system (E_{PHS}) is calculated by Eq. (39) [76].

$$E_{PHS} = \frac{V_{ER-max}\ SE_{PHS}}{N_{PHS}} \tag{39}$$

SE_{PHS} is the specific GHG emissions produced by the construction of the PHS system, and N_{PHS} is the lifetime of the PHS system.

2.3.6.2. BS system. The total annual amount of GHG emissions caused by the use of the BS system (E_{BS}) is calculated based on the $BS_{c\text{-max}}$, the lifetime of the BS system (N_{BS}), and the specific GHG emissions produced by the manufacturing processes of the BS system (SE_{BS}) (Eq. (40)) [77–79]. During the operating process, the BS system has no direct GHG emissions [35,78].

$$E_{BS} = \frac{BS_{c-max}\ SE_{BS}}{N_{BS}} \tag{40}$$

3. Case study

The innovative system with scenarios 1 and 2, as well as the current and conventional systems for DW production from BGW (Section 2.1) are investigated at a reference site in Jordan (Al-Karameh zone, latitude 31.95°, longitude 35.60°). The characteristics of the considered well water are summarized in Table 1.

The electricity generation by the PV system is calculated based on meteorological conditions (hourly values of the global solar radiation, air temperature and wind speed) for the year 2007 (the mean year in a ten-year period from 2007 to 2016) at the reference site. These meteorological data are obtained from the satellite database PVGIS-SARAH [80]. Fig. 3 illustrates the hourly values of the global solar radiation and the air temperature over the year 2007.

The economic project lifetime is set at 25 years [36,81] and the interest rate at 7 % [82]. The rest of this section defines and describes the

Table 1
Characteristics of groundwater [29].

Parameter	Value
Total dissolved solids (NaCl)	5000 mg/L
pH	8
Temperature	25 °C
Depth of BGW table	100 m
Maximum BGW flow rate from well	500 m^3/d

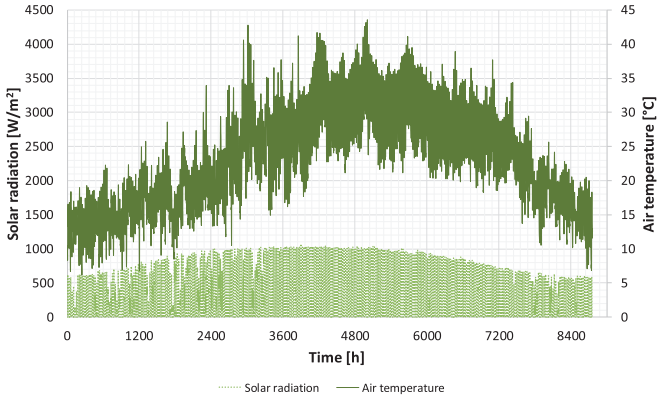

Fig. 3. Hourly values of global solar radiation and air temperature in the year 2007 (mean year) [80].

key assumptions, input parameters and criteria used for the technical modeling, as well as for the economic and GHG emissions analysis for the required components of the examined systems for DW production from BGW. In addition, a sensitivity analysis is defined for important input parameters to evaluate the impact of these parameters on the simulation results.

3.1. Components of examined systems

3.1.1. BWRO plant

In all examined systems, the BWRO plant is designed with a DW production capacity of 100 m^3/d (4.17 m^3/h). However, since in the innovative system the BGW to be stored is pre-treated before it is pumped to the elevated reservoir, the maximum capacity of the pre-treatment process must be adequate for pre-treating the maximum BW flow rate to the elevated reservoir (Section 3.1.6) and the required BW flow rate to the BWRO desalination process (Q_{BWRO}). The latter is assumed to be 25 % of the maximum BW flow rate from the well [29]. In the current and conventional systems, the capacity of the pre-treatment process should only be adequate for pre-treating the Q_{BWRO}. The length and the inner diameter of the well pipe are 100 m and 0.1 m [29].

The specific capital cost of the whole BWRO plant is estimated at 1100 US$/($m^3$/d) [83,84]. In the conventional and current systems, the capital costs for the well pumping station, the pre-treatment process, and the post-treatment process are determined to be 8 %, 0.5 % and 1 % of the total *CAPEX* of the whole BWRO plant, respectively [43]. However, in the innovative system with scenarios 1 and 2, the capacity of the well pumping station and the pre-treatment process are four times the capacity of the well pumping station and the pre-treatment process in the conventional and current systems (Section 3.1.6). Therefore, it is assumed that the capital costs of the well pumping station and the pre-treatment process for the innovative system are four times the capital costs of the well pumping station and the pre-treatment process in the conventional and current systems. The replacement cost of the BWRO membrane elements is determined 765 US$/element [85].

The annual amount of GHG emissions from the whole BWRO plant is assumed to be 14.6 % of the annual amount of GHG emissions caused by the use of the diesel generator to cover the total electric energy demand of the whole BWRO plant [86–89]. This value includes the GHG emissions during the construction (including equipment manufacturing), assembly and operation phases of the whole BWRO plant.

3.1.2. Evaporation ponds

The potential evaporation rates are high in Jordan [90]. At the site of the brine evaporation ponds, the evaporation rate for the freshwater is 2450 mm/year [91,92]. The specific capital cost of the evaporation ponds is estimated at 320 US$/($m^3$/d) [43,93].

3.1.3. PV system

Fixed-tilt crystalline silicon modules with an operational life span of 25 years are simulated to calculate the hourly values of the PV generated electric power [33]. However, the life span of the inverter is only 10 years [94,95]. Within the PV system, the total internal losses are estimated at 14 % [33,80]. The specific costs of the PV modules, the inverter, and the substructure as well as installation (including power cables and controller units) are determined 650 US$/kW, 200 US$/kW, and 300 US$/kW, respectively [45,96–99]. The specific GHG emissions for electricity generation from the PV system are 47.2 g CO_2-eq/kWh [70,100].

3.1.4. Power grid

The application of the net metering scheme in Jordan is allowed for PV systems [101] including water desalination projects driven by PV systems [50]. However, the nominal output of the PV system should be <1 MW [102]. The electricity that the PV system feeds into the national power grid and exceeds the total electricity consumption for the BWRO plant from the national power grid is priced at the levelized cost of electricity from the PV system. For system D (grid), the current electricity price is 0.13 US$/kWh [103]. Since the electricity price is subsidized by the government [104] and may vary significantly over time, the influence of the variation of the electricity price on the UPC_{DW} is investigated. The electricity price is varied between 0 and 1 US$/kWh. In Jordan, the grid losses through the transmission and distribution processes are 13.8 % of the electricity generation [105,106]. The specific GHG emissions related to the electricity generation for the national power grid are 542.5 g CO_2-eq/kWh [50]. Renewable energy systems feeding into the national power grid only 20 % of the total electricity generated in the Jordanian power grid. The rest is generated from fossil fuel energy [51,107,108], although Jordan is a net-fossil energy importing country [69].

3.1.5. Diesel generator

For small diesel generators, the slope coefficient of the generator fuel curve and the intercept coefficient of the generator fuel curve have typical values of 0.246 L/(kW h) and 0.08145 L/(kW h), respectively [54,109]. The specific capital cost of the diesel generator is regarded to be 241 $/kW [110]. The specific costs for the operation and maintenance of the diesel generator typically has a value of 0.05 US$/kWh [55]. The lifetime of the diesel generator and the specific costs for replacement of the diesel generator are equal to 15,000 h [53,54] and 241 $/kW [110], respectively. The current diesel fuel price in Jordan is 1.11 US$/L [111]. Since the diesel fuel price is strongly dependent on the location and may vary significantly over time, the influence of the variation of the diesel fuel price on the UPC_{DW} is investigated. The diesel fuel price is varied between 0 and 3 US$/L. The emission factor for the diesel fuel burned with the diesel generator is 2.69 kg CO_2-eq/L [112,113].

3.1.6. ES system

The main parameters used for the technical modeling, as well as for the economic and GHG emissions analysis for the ES system (PHS system and BS system) are summarized in Table 2.

3.2. Sensitivity analysis

The specific GHG emissions caused by the use of the energy resources and storages of the examined systems can vary depending on the installed power, the storage capacity, production processes, the construction materials used, and the location [78,103,120]. Furthermore, the specific costs of the components of the examined systems mainly depend on the location, the manufacturers, the prices of production materials and the quality of the components [96,116,121]. Therefore, a sensitivity analysis for all examined systems is conducted, where important input parameters used for the economic and GHG emissions analysis are changed by −50 % to +50 %. The sensitivity variables are the specific capital costs of the PV system, the PHS system and the BS system, as well as the specific GHG emissions caused by the PV system, the PHS system, the BS system and the electricity generation for the national power grid.

4. Results and discussion

The results for the economic and GHG emissions analysis of all examined systems are presented, evaluated and discussed in detail in Sections 4.1 and 4.2.

4.1. Economic analysis

4.1.1. Innovative system

The results of the economic analysis of the innovative system are presented individually for scenario 1 and scenario 2.

4.1.1.1. Scenario 1: PV, PHS and BS. In scenario 1, the *CAPEX* and *OPEX* of the entire system as well as the UPC_{DW} are 313,140 US$, 9244 US$/year, and 0.99 US$/m^3, respectively, when only the minimum required nominal output of the PV system of 34 kW is installed. If the $P_{n\text{-}PV}$ is increased by 41.2 %, the UPC_{DW} is reduced to its minimum value ($UPC_{DW\text{-}min}$) of 0.78 US$/m^3 (Fig. 4). The *CAPEX* and *OPEX* of the entire system are reduced by 20.4 % and 22.1 %, respectively. The reason is that by this increasing of the $P_{n\text{-}PV}$, the required electric storage capacity of the BS system is reduced to its minimum value and the $V_{ER\text{-}max}$ is reduced by 82 % (Fig. B.1 in Appendix B). A further increase in the $P_{n\text{-}PV}$ leads to an increase in the *CAPEX* and *OPEX* of the entire system, since the increase in the *CAPEX* and *OPEX* of the PV system is greater than the decrease in the *CAPEX* and *OPEX* of the PHS system. Therefore, the UPC_{DW} is increased.

Table 2
Technical and economic parameter as well as GHG emissions specifications of the storage system.

Main component	Parameter	Value	Reference
PHS system	Maximum flow rate for PHS charging ($Q_{HPPHS\text{-}max}$)	3 Q_{BWRO}	[29]
	Total length (L_{Pi}) and inner diameter (d_{Pi}) of the water pipeline between the elevated reservoir and the BWRO plant	L_{Pi}: 400 m, d_{Pi}: 0.1 m	[29]
	Specific capital cost of the water pipeline between the elevated reservoir and the BWRO plant (SC_{Pi})	17.5 US $/m	[114]
	Specific capital cost of the elevated reservoir (SC_{ER})	27 US$/m^3	[115,116]
	Specific GHG emissions produced by the construction of the PHS system (SE_{PHS})	18 kg CO_2-eq/m^3	[76]
	Lifetime of the PHS system (N_{PHS})	40 years	[59,117]
BS system	Specific capital cost of the storage battery (SC_B):	546.3 US $/kWh	[118]
	Lifetime of the storage battery (N_{BS})	10 years	[26]
	Specific capital cost of the inverter with control units ($SC_{BS\text{-}con}$): StorEdge inverter with HD-wave technology	87.4 US $/kWh	[119]
	Lifetime of the inverter with controller units (SolarEdge)	25 years	[119]
	Specific GHG emissions produced by the manufacturing processes of the BS system (SE_{BS})	172 kg CO_2-eq/kWh	[78]

Q_{BWRO} is the required BW flow rate to the BWRO desalination process.

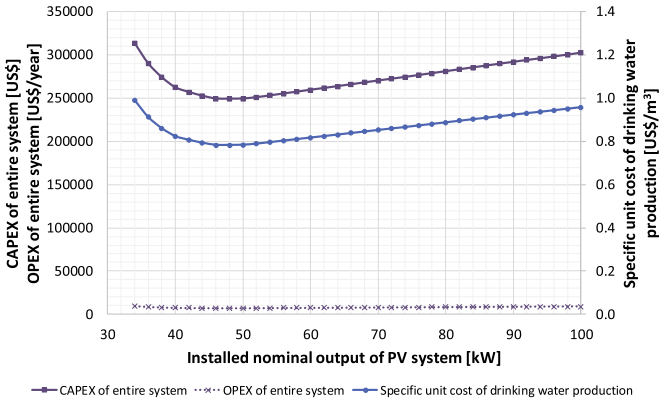

Fig. 4. Drinking water production costs by innovative system with scenario 1 (PV, PHS and BS), depending on the installed nominal output of PV system.

4.1.1.2. Scenario 2: PV, PHS and grid. In scenario 2, the *CAPEX* and *OPEX* of the entire system are 307,030 US$ and 8738 US$/year, respectively, when only the minimum required nominal output of the PV system of 34 kW is installed. The $\Delta EC_{feed\text{-}in}$ and the UPC_{DW} are 129 US$/year and 0.96 US$/m^3. If the $P_{n\text{-}PV}$ is increased by 47 %, the UPC_{DW} is reduced to its minimum value ($UPC_{DW\text{-}min}$) of 0.71 US$/m^3 (Fig. 5). The reason is that by this increasing of the $P_{n\text{-}PV}$, the $V_{ER\text{-}max}$ is reduced by 84 % (Fig. B.1 in Appendix B). Therefore, the *CAPEX* and *OPEX* of the entire system are greatly reduced by 19.6 % and 19.8 %, respectively. Additionally, the surplus PV electricity is fed into the national power grid (Section 2.2.4). A further increase of the $P_{n\text{-}PV}$ has almost no influence on the UPC_{DW}, since the $V_{ER\text{-}max}$ is only very slightly reduced (Fig. B.1 in Appendix B).

4.1.2. State-of-the-art

The results of the economic analysis for the two current systems (system A and system B) are presented below.

4.1.2.1. System A: PV and BS. In system A, the *CAPEX* and *OPEX* of the entire system as well as the UPC_{DW} are 2,397,325 US$, 190,910 US$/year, and 10.87 US$/m^3, respectively, when only the minimum required nominal output of the PV system of 34.5 kW is installed. By increasing the $P_{n\text{-}PV}$

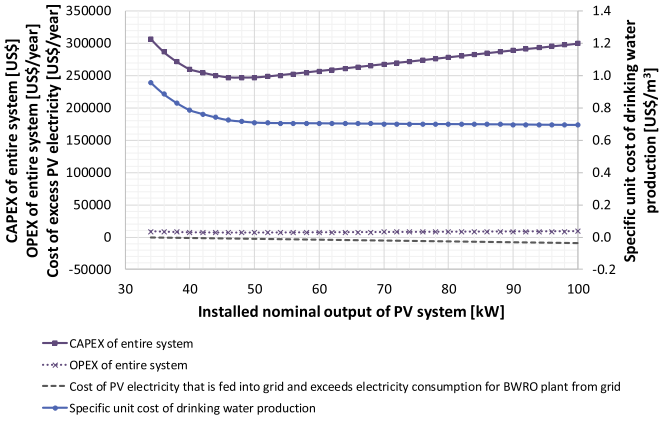

Fig. 5. Drinking water production costs by innovative system with scenario 2 (PV, PHS and grid), depending on the installed nominal output of PV system.

by 27.5 %, the UPC_{DW} is greatly reduced by 78.6 % (Fig. 6). The *CAPEX* and *OPEX* of the entire system are reduced by 76.9 % and 80.4 %, respectively, because the required electric storage capacity of the BS system is greatly reduced by 82.8 % as illustrated in Fig. B.2 in Appendix B. The $UPC_{DW\text{-min}}$ of 1.55 US$/m^3 is achieved by increasing the minimum required nominal output of the PV system by 317.4 %. A further increase in the $P_{n\text{-}PV}$ leads to an increase in the UPC_{DW}, since the increase in the *CAPEX* and *OPEX* of the PV system is greater than the decrease in the *CAPEX* and *OPEX* of the BS system.

4.1.2.2. System B: PV and grid. The *CAPEX* and *OPEX* of the entire system are 155,951 US$ and 5042 US$/year, respectively, when only the minimum required nominal output of the PV system of 33 kW is installed. The $\Delta EC_{feed\text{-}in}$ and the UPC_{DW} are 28 US$/year and 0.5 US$/m^3. The $UPC_{DW\text{-}min}$ is also at the minimum required nominal output of the PV system, since for this system no energy storages are needed. In addition, the W_{pg} is compensated by the $W_{feed\text{-}in}$ at the same price (Section 2.2.4).

4.1.3. Conventional systems

The results of the economic analysis for the two conventional systems (system C and system D) are presented below.

4.1.3.1. System C: diesel generator. In system C, the *CAPEX* of the entire system is 119,688 US$. The *OPEX* of the entire system and the UPC_{DW} with the current price of diesel fuel at the reference site are 28,212 US$/year, and 1.05 US$/m^3, respectively. Fig. 7 illustrates the influence of the variation of the diesel fuel price between 0 and 3 US$/L on the DW production costs. By increasing the diesel fuel price, the UPC_{DW} is increased linearly by 0.01 US$/m^3 for each additional 0.02 US$/L on the diesel fuel price.

4.1.3.2. System D: grid. The *CAPEX* of the entire system is 118,001 US$. The *OPEX* of the entire system and the UPC_{DW} with the current price of electricity from the national power grid at the reference site are 11,212 US$/year, and 0.58 US$/m^3, respectively. Fig. 8 illustrates the influence of the variation of the electricity price between 0 and 1 US$/kWh on the DW production costs. By increasing the electricity price, the UPC_{DW} is increased linearly by 0.03 US$/m^3 for each additional 0.02 US$/kWh on the electricity price.

4.1.4. Comparison of examined systems

In all examined systems with or without grid connection, at the current price of diesel fuel and electricity, the lowest UPC_{DW} of 0.5 US$/m^3 is in system B (PV and grid) (Fig. 9). The reason is that this system does not require any ES. Moreover, the total amount of electricity that the BWRO plant draws from the national power grid is compensated by the electricity that the PV system feeds into the national power grid at the same price. The lowest *CAPEX* of all examined systems is in system D

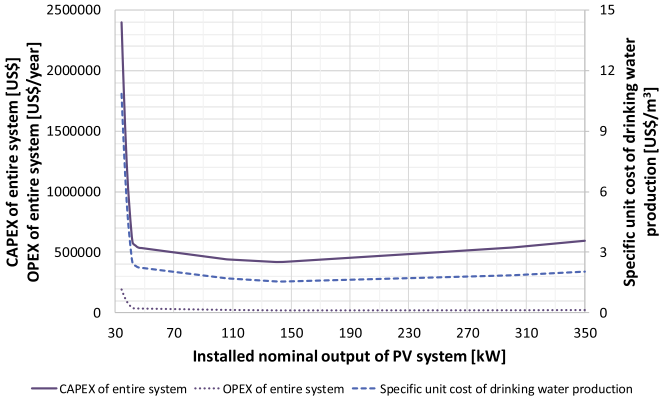

Fig. 6. Drinking water production costs by system A (PV and BS) in dependence on the installed nominal output of PV system.

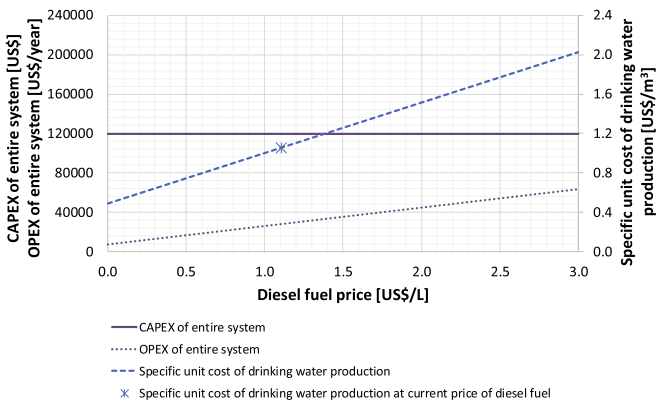

Fig. 7. Drinking water production costs by system C (diesel generator), depending on the diesel fuel price.

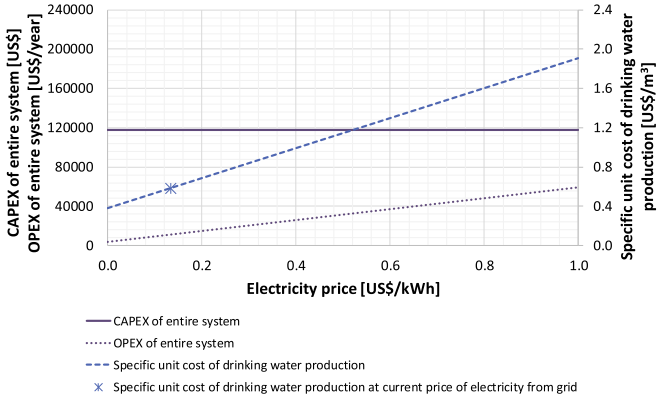

Fig. 8. Drinking water production costs by system D (grid), depending on the electricity price.

(grid), since no PV system and no diesel generator are used. However, the *OPEX* of this system is 122.4 % higher than in system B, since the total electricity consumption of the BWRO plant is covered by the national power grid with the current price of electricity. Therefore, the $UPC_{DW\text{-min}}$ in system D is 16 % higher than in system B. The $UPC_{DW\text{-}min}$ in system D is 17.5 % less than in the innovative system with scenario 2 (PV, PHS and grid) because the price of electricity from the national power grid for DW treatment plants is subsidized by the government. If the price of electricity from the national power grid is equal to or more expensive than 0.22 US$/kWh, the $UPC_{DW\text{-min}}$ in system D will be higher than in scenario 2 (Fig. 10). Thus, for grid connected operation (as in this work: innovative system with scenario 2, system B and system D), the innovative system with scenario 2 will come second after system B (the most economical system) when the price of electricity is equal to or more expensive than 0.22 US$/kWh. The $UPC_{DW\text{-min}}$ in system B is 28.9 % lower than in scenario 2. In addition, the $UPC_{DW\text{-}min}$ in system B remains lower than in system D as long as the price of electricity is more expensive than 0.08 US$/kWh.

The highest *CAPEX* of all examined systems of 418,941 US$ and the highest $UPC_{DW\text{-}min}$ of 1.55 US$/m^3 are in system A (PV and BS) (Fig. 9). The main reason is that system A requires a BS system with a large electric storage capacity of 213.6 kWh. This required storage capacity of the BS system is about 54 times larger than in the innovative system with scenario 1 (PV, PHS and BS). Therefore, the $UPC_{DW\text{-}min}$ in scenario 1 is 49.4 % lower than in system A. Furthermore, the $UPC_{DW\text{-}min}$ in scenario 1 is 25.7 % lower than in system C (diesel generator) at the current price of diesel fuel. The $UPC_{DW\text{-}min}$ in scenario 1 remains less than in system C as long as the diesel fuel price is equal to or more expensive than 0.58 US$/L (Fig. 10). Thus, for off-grid operation (as in this work: innovative system with scenario 1,

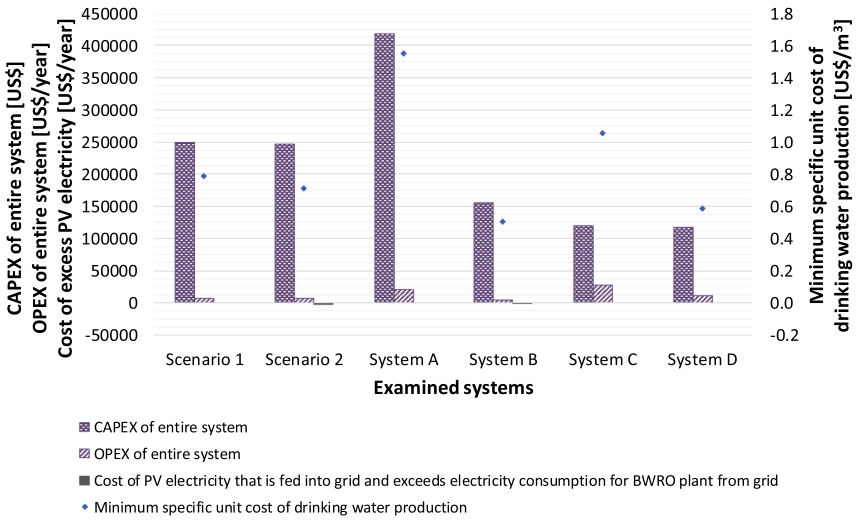

Fig. 9. Minimum drinking water production costs by innovative system with scenario 1 (PV, PHS and BS) and scenario 2 (PV, PHS and grid), as well as by two current systems: system A (PV and BS) and system B (PV and grid). In addition, drinking water production costs by two conventional systems: system C (diesel generator) and system D (grid) at current price of diesel fuel and electricity.

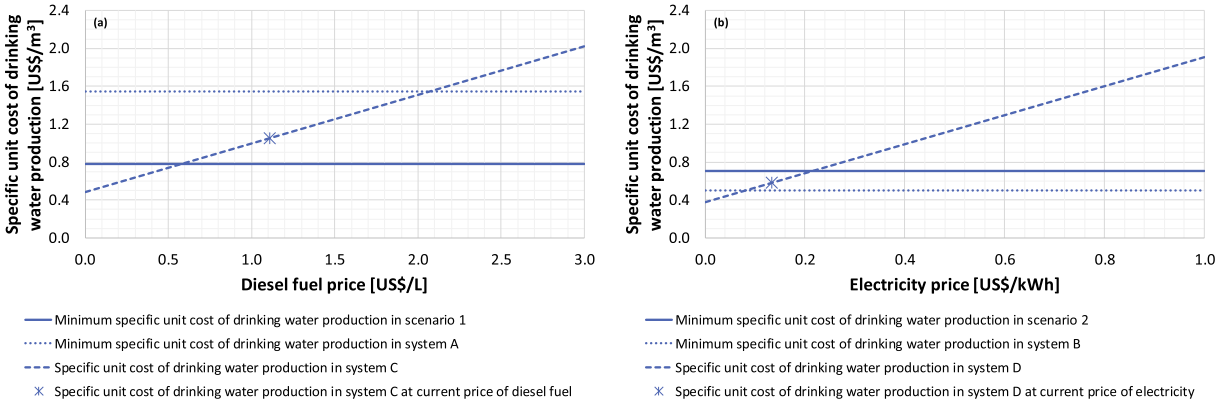

Fig. 10. Comparison of specific unit costs of drinking water production for (a) off-grid operation (innovative system with scenario 1 (PV, PHS and BS), system A (PV and BS), and system C (diesel generator)), depending on the diesel fuel price and for (b) grid connected operation (innovative system with scenario 2 (PV, PHS and grid), system B (PV and grid), and system D (grid)), depending on the electricity price.

system A and system C), the innovative system with scenario 1 is the most economical system for DW production from BGW. Then, system C comes second as long as the diesel fuel price is cheaper than 2.08 US$/L. If the diesel fuel price is equal to or more expensive than 2.08 US$/L, system A will be more economical than system C.

4.1.5. Sensitivity analysis

The results of the sensitivity analysis for the examined systems with off-grid operation: innovative system with scenario 1 (PV, PHS and BS), system A (PV and BS), and system C (diesel generator) are illustrated in Fig. 11. When the specific capital costs of the PV system, the PHS system or the BS system change by −50 % to +50 %, the $UPC_{DW\text{-min}}$ varies between 0.69 US$/m^3 and 0.87 US$/m^3 in scenario 1 and between 1.24 US$/m^3 and 1.86 US$/m^3 in system A. Thus, the innovative system with scenario 1 remains more economical than system A. Furthermore, the $UPC_{DW\text{-min}}$ in scenario 1 is less than in system C as long as the diesel fuel price is equal to or more expensive than 0.76 US$/L.

The change in the specific capital costs of the BS system has a significant impact on the $UPC_{DW\text{-min}}$ in system A compared to scenario 1, as the required storage capacity of the BS system in system A is about 54 times larger than in scenario 1. By decreasing the specific capital costs of the BS system by 50 %, the $UPC_{DW\text{-min}}$ in system A is reduced by 20.2 %. Nevertheless, the $UPC_{DW\text{-}min}$ in scenario 1 is 37.1 % lower than in system A. By increasing the specific capital costs of the PHS system by 50 %, the $UPC_{DW\text{-}min}$ in scenario 1 is increased by 5.1 %. Nevertheless, the $UPC_{DW\text{-}min}$ in scenario 1 is 46.9 % lower than in system A.

Due to the use of the PHS system in scenario 1, a PV system with a nominal output about 66,7 % less than in system A is required in scenario 1 to achieve the $UPC_{DW\text{-}min}$ (Sections 4.1.1.1 and 4.1.2.1). Therefore, the change in the specific capital costs of the PV system has a significant impact on the $UPC_{DW\text{-min}}$ in system A compared to scenario 1. When the specific capital costs of the PV system change by −50 % to +50 %, the $UPC_{DW\text{-min}}$ varies between 0.69 US$/m^3 and 0.87 US$/m^3 in scenario 1 and between 1.28 US$/m^3 and 1.82 US$/m^3 in system A. With this change in the $UPC_{DW\text{-}min}$, the $UPC_{DW\text{-}min}$ in scenario 1 is at least 45.8 % lower than in system A.

Fig. 12 illustrates the results of the sensitivity analysis for the examined systems with grid connected operation: innovative system with scenario 2 (PV, PHS and grid), system B (PV and grid), and system D (grid). When the specific capital costs of the PV system and the PHS system change by −50 % to +50 %, the $UPC_{DW\text{-min}}$ varies between 0.65 US$/m^3 and 0.77 US$/m^3 in scenario 2 and between 0.44 US$/m^3 and 0.57 US$/m^3 in system B. Thus, the system B remains more economical than the innovative system with scenario 2. However, the $UPC_{DW\text{-}min}$ in

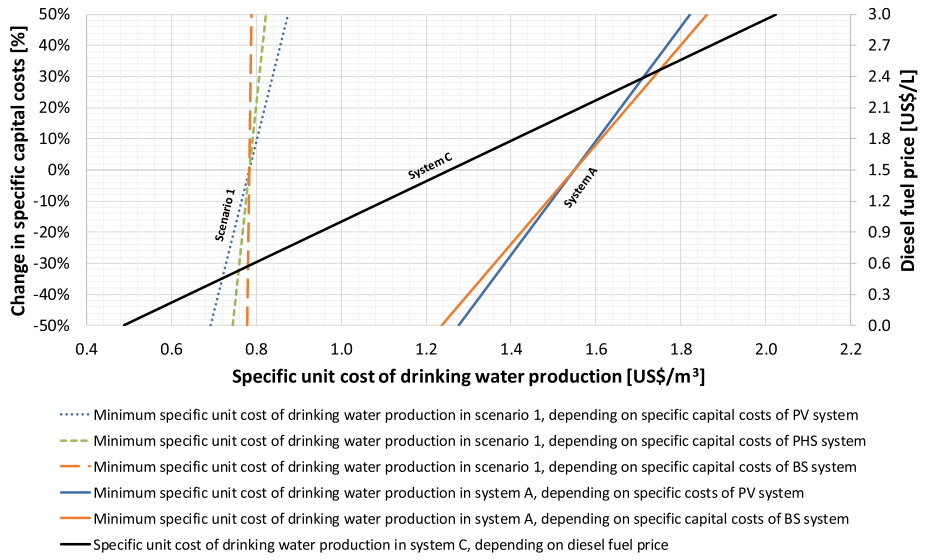

Fig. 11. Impact of change in specific capital costs of PV system, PHS system and BS system, as well as variation of diesel price on specific unit costs of drinking water production of examined systems with off-grid operation: innovative system with scenario 1 (PV, PHS and BS), system A (PV and BS), and system C (diesel generator).

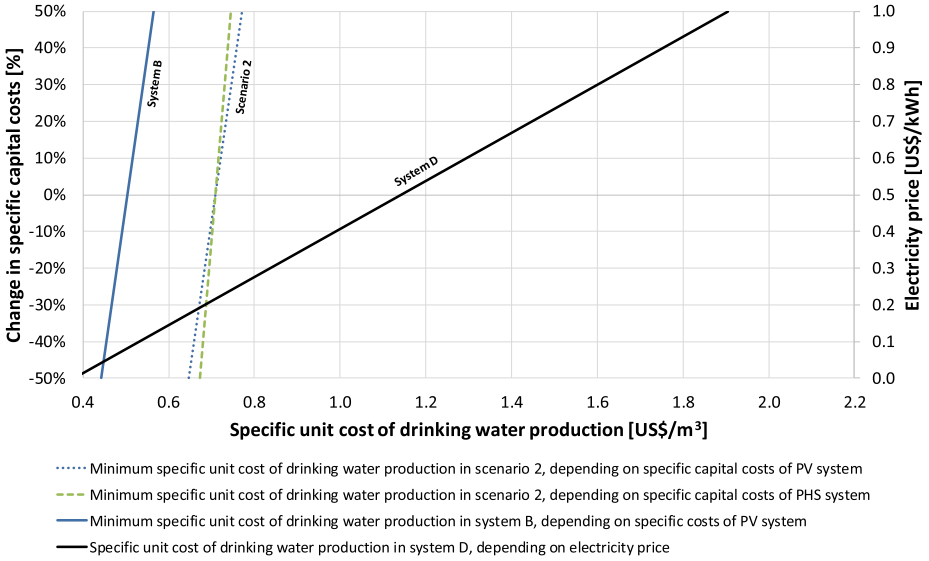

Fig. 12. Impact of change in specific capital costs of PV system and PHS system, as well as variation of electricity price on specific unit costs of drinking water production of examined systems with grid connected operation: innovative system with scenario 2 (PV, PHS and grid), system B (PV and grid), and system D (grid).

scenario 2 is less than in system D as long as the price of electricity is equal to or more expensive than 0.26 US$/kWh.

By increasing the specific capital costs of the PHS system by 50 %, the $UPC_{DW\text{-}min}$ in scenario 2 is increased by 5.2 %. Therefore, the difference between the $UPC_{DW\text{-}min}$ in system B and the $UPC_{DW\text{-}min}$ in scenario 2 increases from 0.2 US$/m^3 to 0.24 US$/m^3. By changing the specific capital costs of the PV system by −50 % to +50 %, the $UPC_{DW\text{-}min}$ varies with a maximum difference of ±8.8 % around the average value of 0.71 US$/m^3 in scenario 2 and with a maximum difference of ±12.3 % around the average value of 0.5 US$/m^3 in system B. With this change in the $UPC_{DW\text{-}min}$ in scenario 2 and system B, the $UPC_{DW\text{-}min}$ in system B is between 26.6 % and 31.6 % lower than the $UPC_{DW\text{-}min}$ in scenario 2.

4.2. GHG emissions analysis

4.2.1. Innovative system

The results of the GHG emissions analysis of the innovative system are presented individually for scenario 1 and scenario 2.

4.2.1.1. Scenario 1: PV, PHS and BS. By installing the minimum required nominal output of the PV system of 34 kW, the TE_{sys} and the SE_{UPW} are 11,509 kg CO_2-eq/year and 0.32 kg CO_2-eq/m^3. If the $P_{n\text{-}PV}$ is increased by 17.6 %, the SE_{UPW} are slightly reduced by 3.2 % to its minimum value of 0.31 kg CO_2-eq/m^3 (Fig. 13). The reason is that by this increasing of the $P_{n\text{-}PV}$, the required electric storage capacity of the BS system is reduced to its minimum value and the $V_{ER\text{-}max}$ is reduced by 58 % (Fig. B.1 in Appendix B). Therefore, the E_{BS} and E_{PHS} are reduced 99.1 kg CO_2-eq/year and 750.3 kg CO_2-eq/year, respectively. However, the E_{PV} is increased only 480,2 kg CO_2-eq/year. Thus, the TE_{sys} is reduced 369.3 kg CO_2-eq/year. A further increase in the $P_{n\text{-}PV}$ leads to an increase in the TE_{sys}, since the increase in the E_{PV} is greater than the decrease in the E_{PHS}. Therefore, the SE_{UPW} are increased (Fig. 13). If the $P_{n\text{-}PV}$ is increased to 48 kW to minimize the UPC_{DW} (Section 4.1.1.1), the SE_{UPW} are increased only slightly by 3 %.

4.2.1.2. Scenario 2: PV, PHS and grid. If only the minimum required

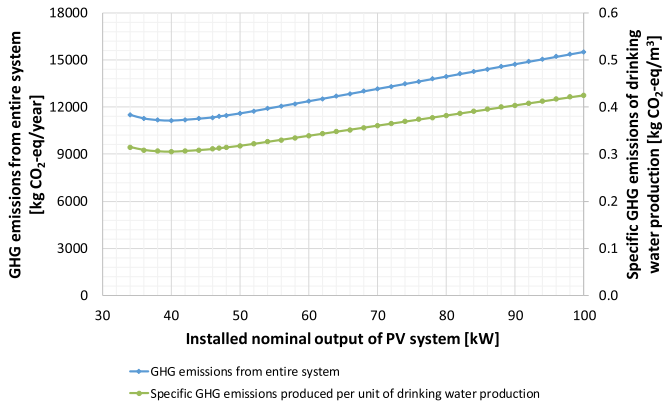

Fig. 13. GHG emissions for drinking water production by innovative system with scenario 1 (PV, PHS and BS), depending on the installed nominal output of PV system.

nominal output of the PV system of 34 kW is installed, the TE_{sys} is 11,343 kg CO_2-eq/year. The $\Delta E_{feed\text{-}in}$ and the SE_{UPW} are 75 kg CO_2-eq/year and 0.31 kg CO_2-eq/m^3, respectively. If the $P_{n\text{-}PV}$ is increased by 47 %, the TE_{sy} is increased only by 190 kg CO_2-eq/year, while the $\Delta E_{feed\text{-}in}$ is increased by 1280 kg CO_2-eq/year. Thus, the SE_{UPW} are reduced to its minimum value of 0.28 kg CO_2-eq/m^3 (Fig. 14). The reason is that by increasing the $P_{n\text{-}PV}$, the $V_{ER\text{-}max}$ is reduced by 84.3 % (Fig. B.1 in Appendix B). Therefore, the E_{PHS} is reduced by 1090 kg CO_2-eq/year. Additionally, the surplus electricity produced by the PV system is fed into the national power grid. A further increase of the $P_{n\text{-}PV}$ has almost no influence on the SE_{UPW}, since the $V_{ER\text{-}max}$ is only very slightly reduced (Fig. B.1 in Appendix B).

4.2.2. State-of-the-art

The results of the GHG emissions analysis for the two current systems (system A and system B) are presented below.

4.2.2.1. System A: PV and BS. By installing the minimum required nominal output of the PV system of 34.5 kW, the TE_{sys} and the SE_{UPW} are 70,882 kg CO_2-eq/year and 1.94 kg CO_2-eq/m^3, respectively. The SE_{UPW} are reduced to its minimum value of 0.57 kg CO_2-eq/m^3 when the $P_{n\text{-}PV}$ is increased by 33.3 % (Fig. 15). The TE_{sys} is reduced by 70.4 %, because the required electric storage capacity of the BS system is greatly reduced (Fig. B.2 in Appendix B). The E_{BS} is reduced 50,848 kg CO_2-eq/year, while the E_{PV} is increased only 920 kg CO_2-eq/year. A further increase in the $P_{n\text{-}PV}$ leads to an increase in the TE_{sys}, since the increase in the E_{PV} is greater than the decrease in the E_{BS}. Therefore, the SE_{UPW} are increased (Fig. 15). If the $P_{n\text{-}PV}$ is increased to 144 kW to minimize the UPC_{DW} (Section 4.1.2.1), the SE_{UPW} are increased only by 7.5 %.

4.2.2.2. System B: PV and grid. By installing the minimum required nominal output of the PV system of 33 kW, the $\Delta E_{feed\text{-}in}$ is only 16 kg CO_2-eq/year. The TE_{sys} and the SE_{UPW} are 9970 kg CO_2-eq/year and 0.27 kg CO_2-eq/m^3, respectively. If the $P_{n\text{-}PV}$ is increased, the SE_{UPW} remain the same. The reason is that system B does not require any ES. In addition, the W_{pg} can be compensated by the $W_{feed\text{-}in}$ even at the minimum required nominal output of the PV system (Section 2.1.2.2).

4.2.3. Conventional systems

The results for GHG emissions from the two conventional systems (system C and system D) are presented below.

4.2.3.1. System C: diesel generator. In system C, the TE_{sys} and the SE_{UPW} are 57,588 kg CO_2-eq/year and 1.58 kg CO_2-eq/m^3, respectively.

4.2.3.2. System D: grid. In system D, the TE_{sys} and the SE_{UPW} are 42,351 kg CO_2-eq/year and 1.16 kg CO_2-eq/m^3, respectively.

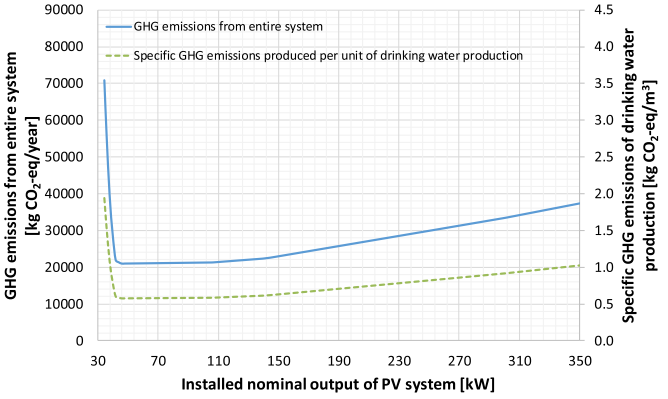

Fig. 15. GHG emissions for drinking water production by system A (PV and BS) in dependence on the installed nominal output of PV system.

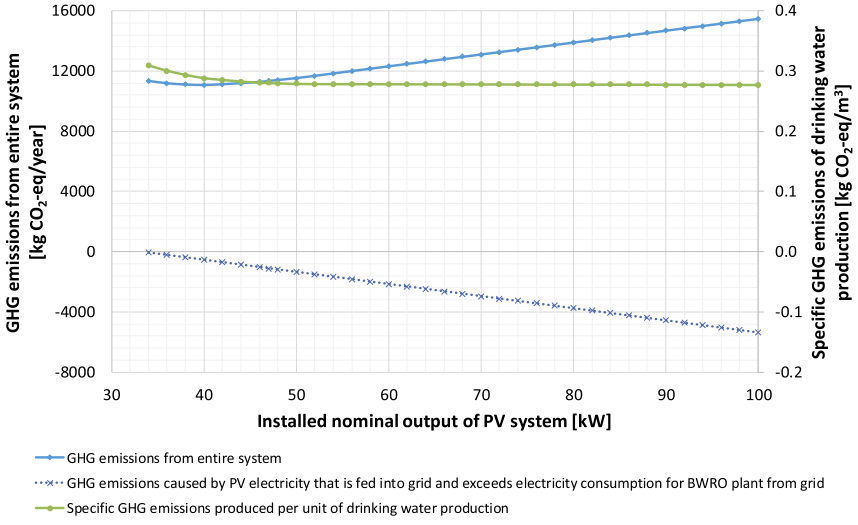

Fig. 14. GHG emissions for drinking water production by innovative system with scenario 2 (PV, PHS and grid), depending on the installed nominal output of PV system.

4.2.4. Comparison of examined systems

In all examined systems with or without grid connection, the lowest SE_{UPW} of 0.27 kg CO_2-eq/m^3 are in system B (PV and grid) (Fig. 16). The reason is that this system does not require any ES. Nevertheless, the total electricity consumption for the operation of the whole BWRO plant is covered by the PV system. The total amount of electricity that the BWRO plant draws from the national power grid (when $EP_{PV} < EP_{BWRO}$) is compensated by the electricity that the PV system feeds into the national power grid (when $EP_{PV} > EP_{BWRO}$) over the course of the year (Section 2.1.2.2).

The minimum specific GHG emissions produced per unit of DW production ($SE_{UPW\text{-}min}$) in system B are only 2.2 % lower than the $SE_{UPW\text{-}min}$ in the innovative system with scenario 2 (PV, PHS and grid) because the E_{PHS} is comparatively low (Table 3). However, the SE_{UPW} in system D (grid) are 325.5 % higher than the $SE_{UPW\text{-}min}$ in system B and 316 % higher than the $SE_{UPW\text{-}min}$ in scenario 2. The reason is that the total electricity demand of the BWRO plant in system D is supplied by the national power grid and about 80 % of the total electricity of the national power grid at the reference site is generated from fossil fuels (Sections 2.1.3.2 and 3.1.4). Therefore, for grid connected operation (as in this work: innovative system with scenario 2, system B and system D), the innovative system with scenario 2 comes second after system B with a very small difference in terms of GHG emissions. System D comes last with a very great difference to scenario 2 in terms of GHG emissions. The minimum annual amount of GHG emissions for DW production from BGW by system B, scenario 2, and system D (without the $\Delta E_{feed\text{-}in}$) are 9954 kg CO_2-eq/year, 10,179 kg CO_2-eq/year, and 42,351 kg CO_2-eq/year, respectively. These minimum values are also achieved when the above systems are designed to minimize the UPC_{DW}. Moreover, the share of the PV electricity that is fed into the national power grid in scenario 2 as well as system B and exceeds the total electricity consumption for the whole BWRO plant from the national power grid (Figs. B.1 and B.2 in Appendix B) contributes to reducing the GHG emissions related to the electricity generation for the national power grid.

The highest $SE_{UPW\text{-}min}$ of all examined systems with or without grid connection is in system C (diesel generator) (Fig. 16), since the total electricity demand of the BWRO plant in this system is completely provided by the diesel generator (Section 2.1.3.1). The $SE_{UPW\text{-}min}$ in system C are 1.58 kg CO_2-eq/m^3. This value is 174.8 % higher than the $SE_{UPW\text{-}min}$ in system A (PV and BS) and 416.9 % higher than the $SE_{UPW\text{-}min}$ in the innovative system with scenario 1 (PV, PHS and BS). The $SE_{UPW\text{-}min}$ in scenario 1 are 46.8 % less than the $SE_{UPW\text{-}min}$ in system A because the required electric storage capacity of the BS system is very small compared to system A (Figs. B.1 and B.2 in Appendix B). Therefore, the E_{BS} in scenario 1 is very low compared to the E_{BS} in system A (Table 4). If the $P_{n\text{-}PV}$ in scenario 1 and system A is increased to minimize the UPC_{DW} (Sections 4.1.1.1 and 4.1.2.1), the $SE_{UPW\text{-}min}$ increase only slightly by 3 % in scenario 1 and by 7.5 % in system A. Thus, for off-grid operation (as in this work: innovative system with scenario 1, system A and system C), the innovative system with scenario 1 is the most ecological system (in terms

Table 3
GHG emissions from energy resources and storages of examined systems with grid connected operation at minimum specific GHG emissions per unit drinking water production.

GHG emissions from energy resources and storages/examined systems	E_{PV}	E_{PHS}	E_{pg}	$\Delta E_{feed\text{-}in}$
	[kg CO_2-eq/year]			
Scenario 2 (PV, PHS and grid)	4002	203	–	−1354
System B (PV and grid)	2641	–	–	−16
System D (grid)	–	–	35,022	–

E_{PV} is the annual amount of GHG emissions from the use of the PV system for electricity generation.
E_{PHS} is the total annual amount of GHG emissions from the use of the PHS system.
E_{pg} is the total annual amount of GHG emissions caused by the BWRO plant's electricity consumption from the national power grid.
$\Delta E_{feed\text{-}in}$ is the annual amount of GHG emissions caused by the share of the PV electricity that is fed into the national power grid and exceeds the total electricity consumption for the whole BWRO plant from the national power grid.

Table 4
GHG emissions from energy resources and storages of examined systems with off-grid operation at minimum specific GHG emissions per unit drinking water production.

GHG emissions from energy resources and storages/examined systems	E_{PV}	E_{PHS}	E_{BS}	E_{DG}
	[kg CO_2-eq/year]			
Scenario 1 (PV, PHS and BS)	3201	543	67	–
System A (PV and BS)	3681	–	9943	–
System C (diesel generator)	–	–	–	50,258

E_{PV}, E_{PHS}, E_{BS}, and E_{DG} are the total annual amount of GHG emissions caused by the use of the PV system, the PHS system, the BS system and the diesel generator, respectively.

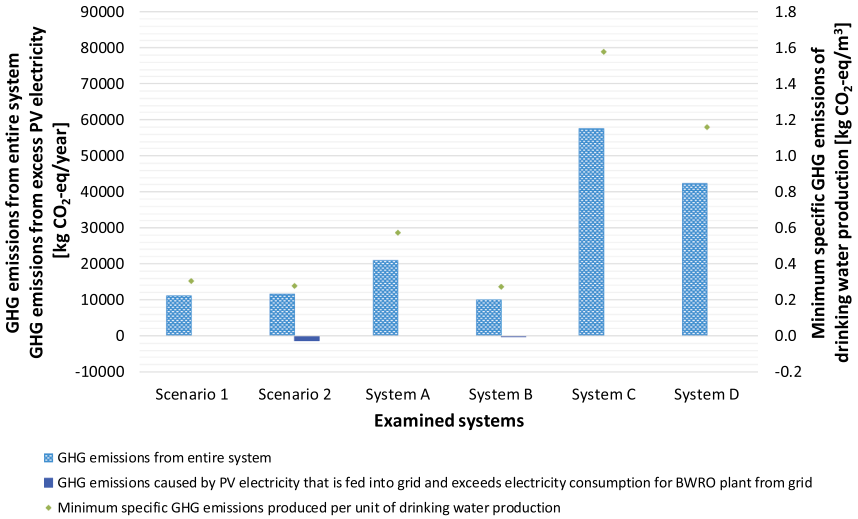

Fig. 16. Minimum GHG emissions for drinking water production by innovative system with scenario 1 (PV, PHS and BS) and scenario 2 (PV, PHS and grid), as well as by two current systems: system A (PV and BS) and system B (PV and grid). In addition, GHG emissions for drinking water production by two conventional systems: system C (diesel generator) and system D (grid).

of GHG emissions) for DW production from BGW when the above systems are designed to minimize the SE_{UPW} or/and the UPC_{DW}. System A then comes second with a great difference to scenario 1 in terms of GHG emissions. System C comes last with a very great difference to system A in terms of GHG emissions. The minimum annual amount of GHG emissions for DW production from BGW by scenario 1, system A and system C is 11,140 kg CO_2-eq/year, 20,954 kg CO_2-eq/year, and 57,588 kg CO_2-eq/year, respectively.

4.2.5. Sensitivity analysis

Fig. 17 illustrates the results of the sensitivity analysis for the examined systems with off-grid operation: innovative system with scenario 1 (PV, PHS and BS) and system A (PV and BS). When the specific GHG emissions caused by the PV system, the PHS system, or the BS system change by −50 % to +50 %, the $SE_{UPW\text{-}min}$ vary between 0.26 kg CO_2-eq/m^3 and 0.35 kg CO_2-eq/m^3 in scenario 1 and between 0.44 kg CO_2-eq/m^3 and 0.71 kg CO_2-eq/m^3 in system A. Thus, the innovative system with scenario 1 remains more ecological (in terms of GHG emissions) than system A. Furthermore, the SE_{UPW} in system C (diesel generator) of 1.58 kg CO_2-eq/m^3 (Section 4.2.3.1) are at least 352 % higher than the $SE_{UPW\text{-}min}$ in scenario 1.

The change in the specific GHG emissions caused by the use of the BS system has a significant impact on the $SE_{UPW\text{-}min}$ in system A compared to scenario 1, as the required electric storage capacity of the BS system in system A is very large compared to scenario 1 (Figs. B.1 and B.2 in Appendix B). By decreasing the specific GHG emissions caused by the use of the BS system by 50 %, the $SE_{UPW\text{-}min}$ are reduced by 23.7 % in system A and only by 0.3 % in scenario 1. Nevertheless, the $SE_{UPW\text{-}min}$ in scenario 1 are 30.5 % lower than in system A. By increasing the specific GHG emissions caused by the use of the PHS system by 50 %, the $SE_{UPW\text{-}min}$ in scenario 1 are increased by 2.4 %. Nevertheless, the $SE_{UPW\text{-}min}$ in scenario 1 are 45.5 % lower than in system A.

When the specific GHG emissions caused by the use of the PV system change by −50 % to +50 %, the $SE_{UPW\text{-}min}$ vary between 0.26 kg CO_2-eq/m^3 and 0.35 kg CO_2-eq/m^3 in scenario 1 and between 0.52 kg CO_2-eq/m^3 and 0.62 kg CO_2-eq/m^3 in system A. With this change in the $SE_{UPW\text{-}min}$, the $SE_{UPW\text{-}min}$ in scenario 1 are at least 44.1 % lower than in system A.

The results of the sensitivity analysis for the examined systems with grid connected operation: innovative system with scenario 2 (PV, PHS and grid), system B (PV and grid), and system D (grid) are illustrated in Fig. 18. When the specific GHG emissions caused by the PV system, the PHS system, or the electricity generation for the national power grid change by −50 % to +50 %, the $SE_{UPW\text{-}min}$ vary between 0.243 kg CO_2-eq/m^3 and 0.315 kg CO_2-eq/m^3 in scenario 2, between 0.237 kg CO_2-eq/m^3 and 0.309 kg CO_2-eq/m^3 in system B, and between 0.68 kg CO_2-eq/m^3 and 1.64 kg CO_2-eq/m^3 in system D. Thus, the innovative system with scenario 2 remains in second place after system B with a small difference in terms of GHG emissions. System D remains in last place with a great difference to scenario 2 in terms of GHG emissions.

By decreasing the specific GHG emissions related to the electricity generation for the national power grid by 50 %, the SE_{UPW} in system D are reduced by 41.3 %. Nevertheless, the SE_{UPW} in system D are 144 % higher than the $SE_{UPW\text{-}min}$ in scenario 2 and 149.5 % higher than the $SE_{UPW\text{-}min}$ in system B. By increasing the specific GHG emissions caused by the use of the PHS system by 50 %, the $SE_{UPW\text{-}min}$ in scenario 2 become 3.3 % higher than the $SE_{UPW\text{-}min}$ in system B.

When the specific GHG emissions caused by the use of the PV system change by −50 % to +50 %, the $SE_{UPW\text{-}min}$ vary with a maximum difference of ±13 % around the average value of 0.28 kg CO_2-eq/m^3 in scenario 2 and with a maximum difference of ±13.2 % around the average value of 0.27 kg CO_2-eq/m^3 in system B. With this change in the $SE_{UPW\text{-}min}$, the $SE_{UPW\text{-}min}$ in system B are between 2.1 % and 2.4 % lower than the $SE_{UPW\text{-}min}$ in scenario 2.

5. Conclusions

The innovative system for a BWRO plant powered by a PV system as a main energy source and a PHS system as an intermediate storage offers a competitive solution for providing DW from BGW. To discuss and evaluate the future role for this innovative system in the BWRO desalination market, this paper economically assessed the entire system with two power supply scenarios: scenario 1 (PV, PHS and BS) and scenario 2 (PV, PHS and grid), as well as analyzed its GHG emissions. Thereafter, this system was compared with two current systems for BWRO desalination powered by a PV system with (BS system or power grid) as the state-of-the-art, and two systems for BWRO desalination powered by a conventional energy source (diesel generator or power grid). The

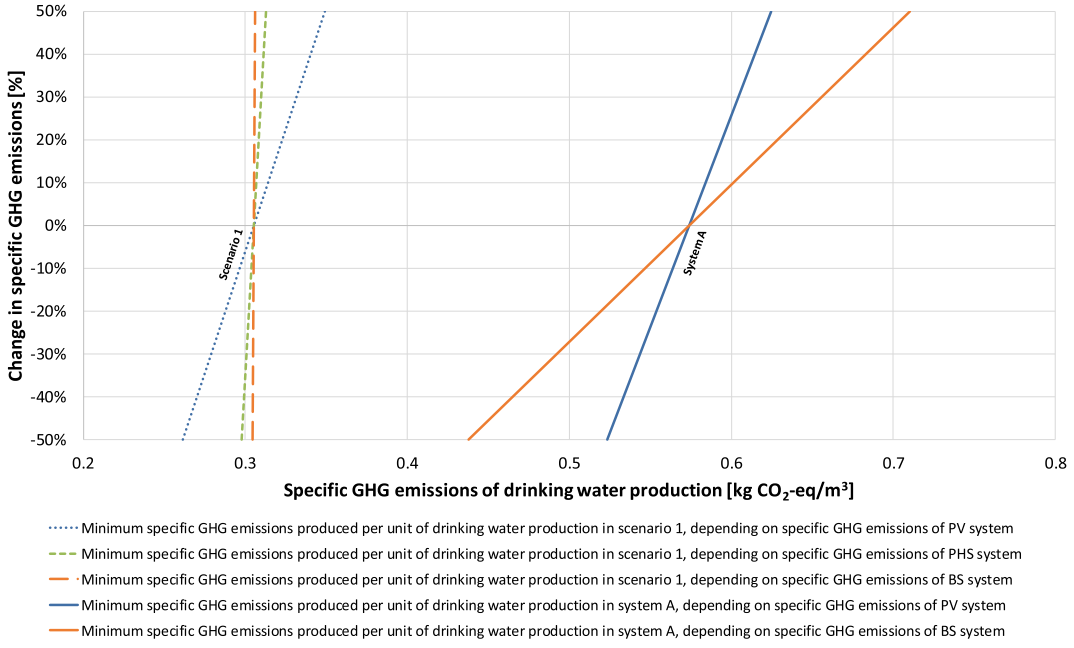

Fig. 17. Impact of change in specific GHG emissions caused by PV system, PHS system and BS system on specific GHG emissions produced per unit of drinking water production of examined systems with off-grid operation: innovative system with scenario 1 (PV, PHS and BS), system A (PV and BS).

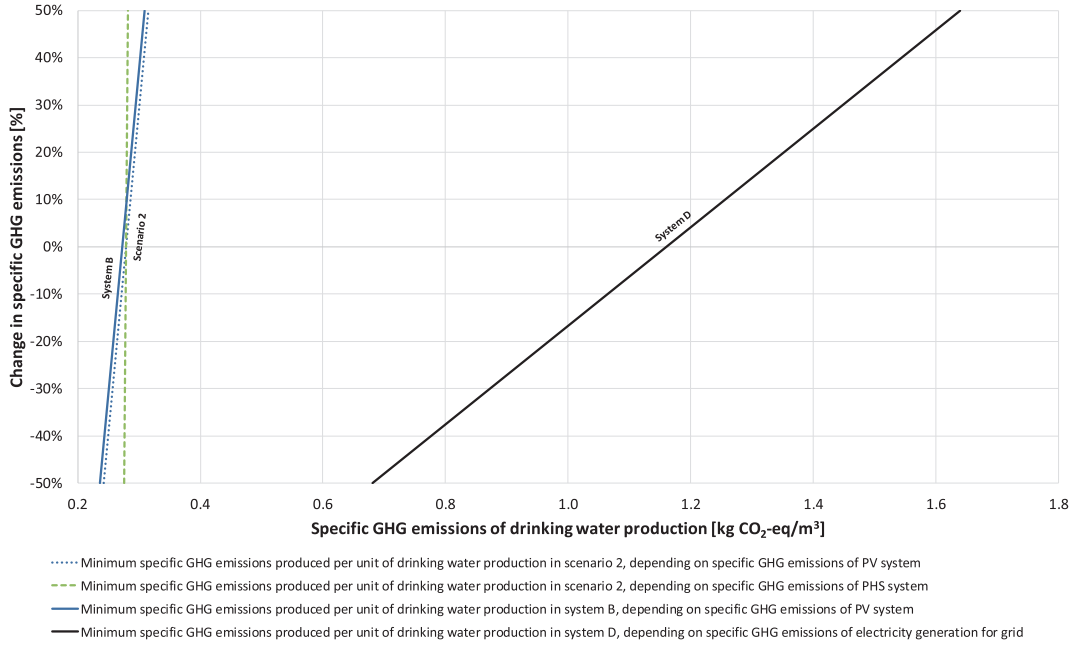

Fig. 18. Impact of change in specific GHG emissions caused by PV system, PHS system, and electricity generation for national power grid on specific GHG emissions produced per unit of drinking water production of examined systems with grid connected operation: innovative system with scenario 2 (PV, PHS and grid), system B (PV and grid), and system D (grid).

innovative system as well as the selected current and conventional systems were simulated and investigated under the same framework conditions. Furthermore, the same specific capital costs and the same specific GHG emissions were considered for the components of the examined systems. By evaluating and comparing the simulation results, the following outcomes were obtained.

- The $UPC_{DW\text{-min}}$ in the innovative system with scenario 1 is 49.4 % lower than in the current system (PV and BS), since the required storage capacity of the BS system in this current system is about 54 times larger than in the innovative system with scenario 1. In addition, the $UPC_{DW\text{-min}}$ in scenario 1 is 25.7 % lower than in the conventional system (diesel generator) at the current price of diesel fuel. Moreover, the $UPC_{DW\text{-}min}$ in scenario 1 remains less than in the conventional system as long as the diesel fuel price is equal to or more expensive than 0.58 US$/L. Thus, in remote off-grid areas, the innovative system with scenario 1 is the most economical system for DW production from BGW compared to the other examined systems. Then, the conventional system (diesel generator) comes second as long as the diesel fuel price is cheaper than 2.08 US$/L. If the diesel fuel price is equal to or more expensive than 2.08 US$/L, the current system (PV and BS) will be more economical than the conventional system (diesel generator).
- For grid connected operation, the current system (PV and grid) is the most economical system for DW production from BGW compared to the innovative system with scenario 2 and the conventional system (grid) at the current price of electricity from the national power grid. The innovative system with scenario 2 comes second after this current system when the price of electricity is equal to or more expensive than 0.22 US$/kWh. The $UPC_{DW\text{-min}}$ in the current system is 28.9 % lower than in the innovative system with scenario 2. The $UPC_{DW\text{-}min}$ in the current system (PV and grid) remains lower than in the conventional system (grid) as long as the price of electricity is more expensive than 0.08 US$/kWh.
- The $SE_{UPW\text{-}min}$ in the innovative system with scenario 1 are 0.31 kg CO_2-eq/m^3. This value is 46.8 % less than the $SE_{UPW\text{-}min}$ in the current system (PV and BS). Additionally, the SE_{UPW} in the conventional system (diesel generator) are 416.9 % higher than in the innovative system with scenario 1. If the installed nominal output of the PV system in scenario 1 and the current system (PV and BS) is increased to minimize the UPC_{DW}, the $SE_{UPW\text{-}min}$ increase only slightly by 3 % in scenario 1 and by 7.5 % in the current system. Thus, in remote off-grid areas, the innovative system with scenario 1 is the most ecological system (in terms of GHG emissions) for DW production from BGW when the examined systems are designed to minimize the SE_{UPW} or/and the UPC_{DW}.
- For grid connected operation, the innovative system with scenario 2 comes second after the current system (PV and grid) with a small difference in terms of GHG emissions. The $SE_{UPW\text{-}min}$ in this current system are only 2.2 % lower than in scenario 2 because the GHG emissions from the use of the PHS system in scenario 2 are comparatively low. However, the SE_{UPW} in the conventional system (grid) are 316 % higher than the $SE_{UPW\text{-}min}$ in scenario 2. The $SE_{UPW\text{-}min}$ in scenario 2 are only 0.28 kg CO_2-eq/m^3. Furthermore, this value and the $SE_{UPW\text{-}min}$ in the current system (PV and grid) are also achieved when these two systems are designed to minimize the UPC_{DW}.

For all examined systems, a sensitivity analysis was also conducted to evaluate the impact of changes in the specific capital costs and GHG emissions for energy resources and storages of the examined systems on the results.

- When the specific capital costs of the PV system, the PHS system or the BS system change by −50 % to +50 %, the innovative system with scenario 1 remains the most economical system for DW production from BGW compared to the other examined systems with off-grid operation. However, only where the diesel fuel price is equal to or more expensive than 0.76 US$/L. For grid connected operation, the innovative system with scenario 2 remains in second place after the current system (PV and grid) when the price of electricity is equal to or more expensive than 0.26 US$/kWh.
- When the specific GHG emissions caused by the PV system, the PHS system, the BS system, or the electricity generation for the national power grid change by −50 % to +50 %, the innovative system with scenario 1 remains the most ecological system (in terms of GHG

emissions) for DW production from BGW compared to the other examined systems with off-grid operation. For grid connected operation, the innovative system with scenario 2 remains in second place after the current system (PV and grid) with a small difference in terms of GHG emissions. The conventional system (grid) remains in last place with a great difference to scenario 2 in terms of GHG emissions.

CRediT authorship contribution statement

Anas Sanna: Conceptualization, Methodology, Software, Formal analysis, Resources, Data curation, Writing – original draft, Visualization, Investigation, Validation, Writing – review & editing. **Wolfgang Streicher:** Supervision, Writing – review & editing.

Declaration of competing interest

The authors declare that they have no known competing financial interests or personal relationships that could have appeared to influence the work reported in this paper.

Data availability

Data will be made available on request.

Appendix A. Technical modeling: state-of-the-art

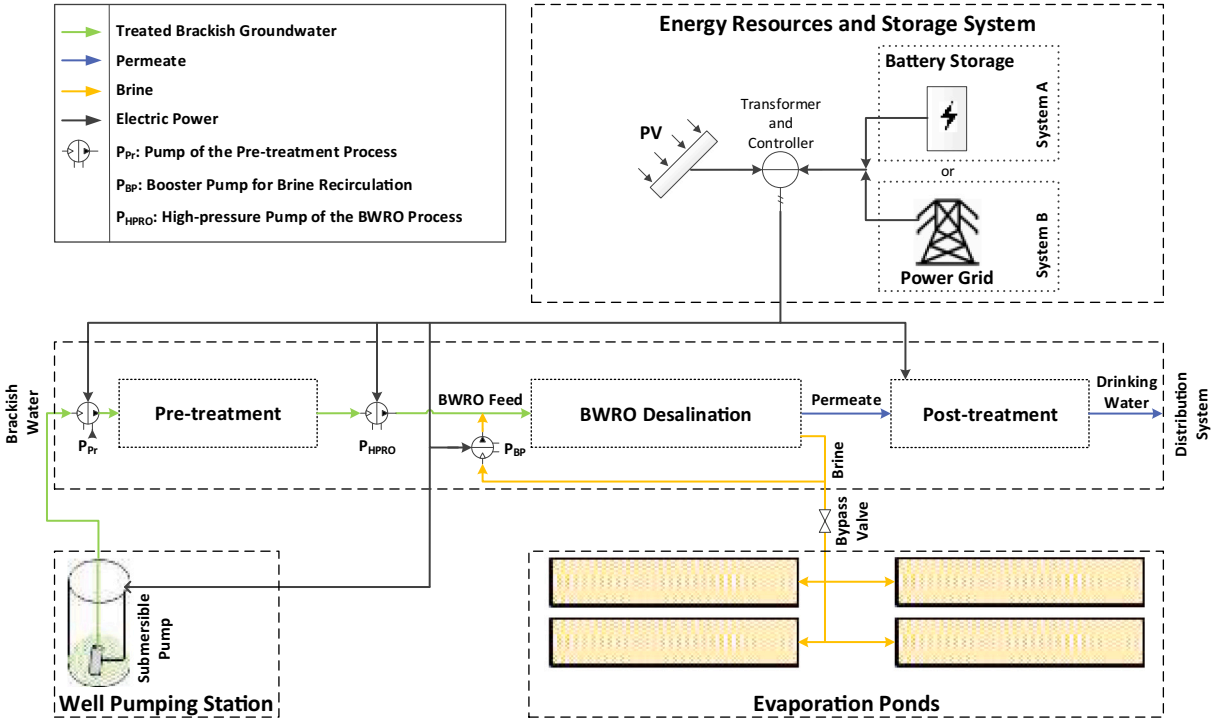

Fig. A.1. Schematic diagram for drinking water production by a BWRO plant powered by PV and BS (system A) or by PV and grid (system B).

Appendix B. Results: technical modeling

The results for the technical modeling of the BWRO plant, evaporation ponds, PV system, PHS system, and BS system are evaluated and discussed in detail in the prior paper [29]. The EP_{BWRO} is 6.35 kW when the BW flow rate from the groundwater well is equal to the Q_{BWRO}. The total daily energy consumption of the whole BWRO plant is 152.5 kWh/d.

Figs. B.1 and B.2 illustrate the effect of increasing the $P_{n\text{-}PV}$ on the required storage capacity of the energy storages (BS system and/or PHS system) in scenario 1 (PV, PHS and BS), scenario 2 (PV, PHS and grid) and system A (PV and BS), as well as on the electricity exchange between the national power grid and the entire system in scenario 2 and system B (PV and grid).

For system C (diesel generator), a diesel generator with a rated output of 7 kW is required. The annual fuel consumption is 18,688 L/year. In system D (grid), the W_{pg} is 55,667 kWh/year.

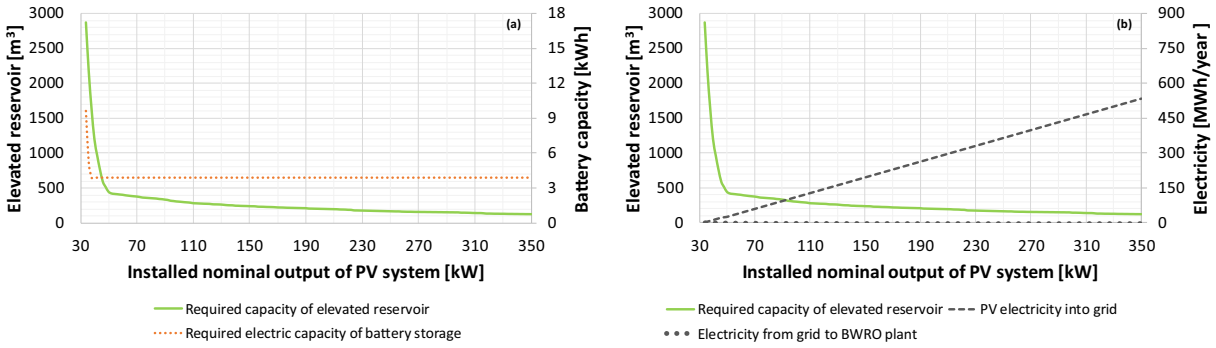

Fig. B.1. Effect of nominal output of PV system on (a) required storage capacity of PHS system as well as BS system in scenario 1 (PV, PHS and BS) and (b) required storage capacity of PHS system as well as electricity exchange between national power grid and entire system in scenario 2 (PV, PHS and grid).

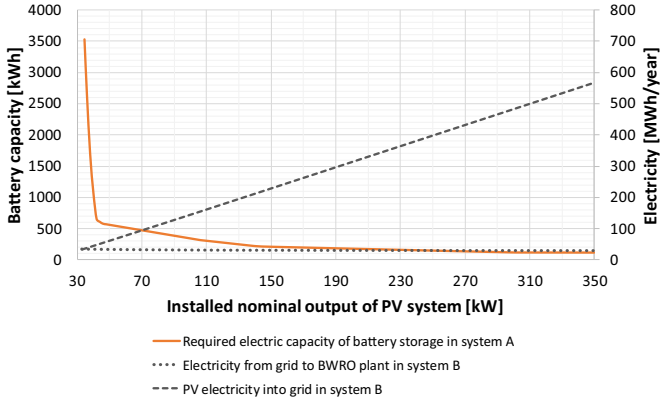

Fig. B.2. Effect of nominal output of PV system on required electric storage capacity of BS system in system A (PV and BS) and electricity exchange between national power grid and system B (PV and grid).

Nomenclature

Acronyms

BGW	brackish groundwater
BS	battery storage
BW	brackish water
DW	drinking water
ES	energy storage
CO_2-eq	carbon dioxide equivalent
GHG	greenhouse gas
PHS	pumped hydro storage
PV	photovoltaic
RO	reverse osmosis
SW	seawater

Variables

$BS_{c\text{-}max}$	maximum electric storage capacity of the BS system (kWh)
C_B	capital cost of the storage battery (US$)
C_{ch}	annual chemical cost for the BWRO plant (US$/year)
C_{DF}	annual cost of diesel fuel required for the operation of the diesel generator (US$/year)
C_{eci}	total costs for the electrical equipment, the controller units, and the installation for the PHS system (US$)
C_{ER}	capital cost of the elevated reservoir (US$)
C_{HPPHS}	capital cost of the high-pressure pump of the PHS system (US$)
C_{ins}	annual insurance cost for the BWRO plant (US$/year)
C_{lab}	annual labor cost for the BWRO plant (US$/year)
C_m	total capital cost of the BWRO membranes (US$)
C_{main}	annual maintenance cost for the BWRO plant (US$/year)
C_{Pi}	capital cost of the water pipeline between the BWRO plant and the elevated reservoir (US$)
$C_{PV\text{-}i}$	capital cost of the inverter for the PV system (US$)
$C_{r\text{-}B}$	annual replacement cost of the storage battery (US$/year)

$C_{r\text{-}DG}$ annual replacement cost of the diesel generator (US$/year)
$C_{r\text{-}PV\text{-}i}$ annual replacement cost of the inverter for the PV system (US$/year)
$C_{r\text{-}m}$ annual replacement cost of the BWRO membranes (US$/year)
$CAPEX$ capital expenditure (US$)
$CAPEX_{BS}$ *CAPEX* of the BS system (US$)
$CAPEX_{BWRO}$ *CAPEX* of the whole BWRO plant (US$)
$CAPEX_{DG}$ *CAPEX* of the diesel generator (US$)
$CAPEX_{EP}$ *CAPEX* of the evaporation ponds (US$)
$CAPEX_{PHS}$ *CAPEX* of the PHS system (US$)
$CAPEX_{PV}$ *CAPEX* of the PV system (US$)
$CAPEX_{sys}$ *CAPEX* of the entire system (US$)
d_{Pi} inner diameter of the water pipeline between the BWRO plant and the elevated reservoir (m)
E_{BS} annual amount of GHG emissions from the use of the BS system (kg CO_2-eq/year)
E_{BWRO} annual amount of GHG emissions from the whole BWRO plant (kg CO_2-eq/year)
E_{DG} annual amount of GHG emissions from the use of the diesel generator (kg CO_2-eq/year)
E_{pg} annual amount of GHG emissions caused by the BWRO plant's electricity consumption from the national power grid (kg CO_2-eq/year)
E_{PHS} annual amount of GHG emissions from the use of the PHS system (kg CO_2-eq/year)
E_{PV} annual amount of GHG emissions from the use of the PV system for electricity generation (kg CO_2-eq/year)
EC_{pg} annual cost of electricity that the BWRO plant draws from the national power grid (US$/year)
EF_{DG} emission factor for the diesel fuel burned with the diesel generator (kg CO_2-eq/L)
EP_{BPPo} electric power consumption of the brine recirculation pump, the post-treatment process, and the disinfection of the BW stored in the elevated reservoir (kW)
EP_{BWRO} electric power consumption of the whole BWRO plant (kW)
EP_{DG} electric power produced by the diesel generator (kW)
$EP_{feed\text{-}in}$ electric feed-in power into the national power grid (kW)
EP_{pg} electric power consumption from the national power grid (kW)
EP_{PV} electric power produced by the PV system (kW)
F_{DG} hourly fuel consumption of the diesel generator (L/h)
f_i intercept coefficient of the generator fuel curve (L/(kW h))
f_s slope coefficient of the generator fuel curve (L/(kW h))
Ir interest rate (−)
L_{Pi} total length of the water pipeline between the BWRO plant and the elevated reservoir (m)
$LCOE_{PV}$ levelized cost of electricity from the PV system (US$/kWh)
LF_{TD} factor for transmission and distribution losses (−)
n economic project lifetime (year)
N_{BS} lifetime of the BS system (year)
N_{DG} lifetime of the diesel generator (h)
N_{PHS} lifetime of the PHS system (year)
No_B number of the storage batteries to be replaced over lifetime of the project (−)
$No_{PV\text{-}i}$ number of the inverters to be replaced over lifetime of the project (−)
OM_{BS} costs for the operation and maintenance of the BS system (US$/year)
OM_{DG} costs for the operation and maintenance of the diesel generator (US$/year)
OM_{PV} costs for the operation and maintenance of the PV system (US$/year)
$OPEX$ operating expenditure (US$/year)
$OPEX_{BS}$ *OPEX* of the BS system (US$/year)
$OPEX_{BWRO}$ *OPEX* of the whole BWRO plant (US$/year)
$OPEX_{DG}$ *OPEX* of the diesel generator (US$/year)
$OPEX_{EP}$ *OPEX* of the evaporation ponds (US$/year)
$OPEX_{PHS}$ *OPEX* of the PHS system (US$/year)
$OPEX_{PV}$ *OPEX* of the PV system (US$/year)
$OPEX_{sys}$ *OPEX* of the entire system for DW production from BGW (US$/year)
P_{DF} diesel fuel price (US$/L)
$P_{HPPHS\text{-}max}$ maximum operating pressure of the high-pressure pump of the PHS system (bar)
$P_{n\text{-}PV}$ installed nominal output of the PV system (kW)
$P_{r\text{-}DG}$ rated output of the diesel generator (kW)
PE_{pg} price of electricity from the national power grid (US$/kWh)
$Q_{B\text{-}EP}$ flow rate of brine from the BWRO desalination process into the evaporation ponds (m^3/h)
Q_{BWRO} required BW flow rate to the BWRO desalination process (m^3/h)
Q_{DW} flow rate of DW produced by the BWRO plant (m^3/h)
Q_{Feed} flow rate of feed water to the BWRO membranes (m^3/h)
$Q_{HPPHS\text{-}max}$ maximum flow rate for PHS charging (m^3/h)
SC_B specific capital cost of the storage battery (US$/kWh)
$SC_{BS\text{-}con}$ specific capital cost of the inverter with control units for the BS system (US$/kWh)
SC_{BWRO} specific capital cost of the whole BWRO plant (US$/($m^3$/d))
SC_{DG} specific capital cost of the diesel generator (US$/kW)
SC_{EP} specific capital cost of the evaporation ponds (US$/($m^3$/d))

SC_{ER} specific capital cost of the elevated reservoir (US$/m^3)
$SC_{OM\text{-}DG}$ specific cost for the operation and maintenance of the diesel generator (US$/h)
SC_{Pi} specific capital cost of the water pipeline between the BWRO plant and the elevated reservoir (US$/m)
$SC_{PV\text{-}i}$ specific costs of the inverter for the PV system (US$/kW)
$SC_{PV\text{-}m}$ specific costs of the PV modules (US$/kW)
$SC_{PV\text{-}si}$ specific costs for the substructure and installation of the PV system (US$/kW)
$SC_{r\text{-}DG}$ specific costs for replacement of the diesel generator (US$/kW)
SE_{BS} specific GHG emissions produced by the manufacturing processes of the BS system (kg CO_2-eq/kWh)
SE_{pg} specific GHG emissions related to the electricity generation for the national power grid (kg CO_2-eq/kWh)
SE_{PHS} specific GHG emissions produced by the construction of the PHS system (kg CO_2-eq/m^3)
SE_{PV} specific GHG emissions for electricity generation from the PV system (kg CO_2-eq/kWh)
SE_{UPW} specific GHG emissions produced per unit of DW production (kg CO_2-eq/m^3)
$SE_{UPW\text{-}min}$ minimum specific GHG emissions produced per unit of DW production (kg CO_2-eq/m^3)
$ST_{PV\text{-}surplus}$ specific tariff for purchasing surplus PV electricity by the distribution company (US$/kWh)
t_{BWRO} operating time of the BWRO plant (h)
t_{DG} operating time of the diesel generator (h)
$t_{feed\text{-}in}$ feed-in time of PV electricity into the national power grid (h)
t_{pg} time of electricity consumption from the national power grid (h)
t_{PV} operating time of the PV system (h)
TE_{sys} total annual amount of GHG emissions from the entire system (kg CO_2-eq/year)
UPC_{DW} specific unit cost of DW production (US$/m^3)
$UPC_{DW\text{-}min}$ minimum specific unit cost of DW production (US$/m^3)
$V_{ER\text{-}max}$ maximum storage capacity of the elevated reservoir (m^3)
$W_{feed\text{-}in}$ annual amount of electricity fed into the national power grid from the PV system (kWh/year)
W_{pg} annual amount of electricity that the BWRO plant draws from the national power grid (kWh/year)

Greek letters

$\Delta E_{feed\text{-}in}$ annual amount of GHG emissions caused by the share of the PV electricity that is fed into the national power grid and exceeds the total electricity consumption for the whole BWRO plant from the national power grid (kg CO_2-eq/year)
$\Delta EC_{feed\text{-}in}$ annual cost of the share of the PV electricity that is fed into the national power grid and exceeds the total electricity consumption for the whole BWRO plant from the national power grid (US$/year)

References

[1] A. Zapata-Sierra, M. Cascajares, A. Alcayde, F. Manzano-Agugliaro, Worldwide research trends on desalination, Desalination 519 (2021), 115305, https://doi.org/10.1016/j.desal.2021.115305.
[2] IDA, GWI DesalData, IDA Desalination and Reuse Handbook 2021–2022: Water Desalination Report. https://idadesal.org/e-library/ida-water-security-handbook/, 2022.
[3] J. Bundschuh, M. Kaczmarczyk, N. Ghaffour, B. Tomaszewska, State-of-the-art of renewable energy sources used in water desalination: present and future prospects, Desalination 508 (2021), 115035, https://doi.org/10.1016/j.desal.2021.115035.
[4] European Commission and the European Environment Agency, Climate-ADAPT, Desalination. https://climate-adapt.eea.europa.eu/en/metadata/adaptation-options/desalinisation, 2023 (accessed 21 May 2023).
[5] Global Water Intelligence, Desalination: tapping into the oceans with desalination. https://www.globalwaterintel.com/articles/topic/desalination, 2022. (Accessed 21 May 2023).
[6] A. Panagopoulos, Water-energy nexus: desalination technologies and renewable energy sources, Environ. Sci. Pollut. Res. Int. 28 (2021) 21009–21022, https://doi.org/10.1007/s11356-021-13332-8.
[7] A. Panagopoulos, K.-J. Haralambous, Environmental impacts of desalination and brine treatment - challenges and mitigation measures, Mar. Pollut. Bull. 161 (2020), 111773, https://doi.org/10.1016/j.marpolbul.2020.111773.
[8] H. Nassrullah, S.F. Anis, R. Hashaikeh, N. Hilal, Energy for desalination: a state-of-the-art review, Desalination 491 (2020), 114569, https://doi.org/10.1016/j.desal.2020.114569.
[9] IPCC, Climate Change 2013: The Physical Science Basis: Contribution of Working Group I to the Fifth Assessment Report of the Intergovernmental Panel on Climate Change, 2013.
[10] A. Sanna, M. Kaltschmitt, M. Ernst, PV-betriebene Umkehrosmoseanlage zur Meerwasserentsalzung – Modellierung und Analyse verschiedener Energieversorgungsvarianten, Chem. Ing. Tech. 91 (2019) 1853–1873, https://doi.org/10.1002/cite.201900095.
[11] C.-S. Karavas, K.G. Arvanitis, G. Papadakis, Optimal technical and economic configuration of photovoltaic powered reverse osmosis desalination systems operating in autonomous mode, Desalination 466 (2019) 97–106, https://doi.org/10.1016/j.desal.2019.05.007.
[12] B. Rahimi, H. Shirvani, A.A. Alamolhoda, F. Farhadi, M. Karimi, A feasibility study of solar-powered reverse osmosis processes, Desalination 500 (2021), 114885, https://doi.org/10.1016/j.desal.2020.114885.
[13] B. Anand, R. Shankar, S. Murugavelh, W. Rivera, K. Midhun Prasad, R. Nagarajan, A review on solar photovoltaic thermal integrated desalination technologies, Renew. Sust. Energ. Rev. 141 (2021), 110787, https://doi.org/10.1016/j.rser.2021.110787.
[14] M. Roggenburg, D.M. Warsinger, H. Bocanegra Evans, L. Castillo, Combatting water scarcity and economic distress along the US-Mexico border using renewable powered desalination, Appl. Energy 291 (2021), 116765, https://doi.org/10.1016/j.apenergy.2021.116765.
[15] C.-S. Karavas, E. Dimitriou, A.T. Balafoutis, D. Manolakos, G. Papadakis, Development of a computational tool for the design of seawater reverse osmosis desalination systems powered by photovoltaics for crop irrigation, Green Energy Sustain (2022) 1–22, https://doi.org/10.47248/ges2202010001.
[16] V.G. Gude, Use of exergy tools in renewable energy driven desalination systems, Therm. Sci. Eng. Prog. 8 (2018) 154–170, https://doi.org/10.1016/j.tsep.2018.08.012.
[17] J. Eke, A. Yusuf, A. Giwa, A. Sodiq, The global status of desalination: an assessment of current desalination technologies, plants and capacity, Desalination 495 (2020), 114633, https://doi.org/10.1016/j.desal.2020.114633.
[18] S.M. Shalaby, S.W. Sharshir, A.E. Kabeel, A.W. Kandeal, H.F. Abosheiasha, M. Abdelgaied, M.H. Hamed, N. Yang, Reverse osmosis desalination systems powered by solar energy: preheating techniques and brine disposal challenges – a detailed review, Energy Convers. Manag. 251 (2022), 114971, https://doi.org/10.1016/j.enconman.2021.114971.
[19] H.R. Lotfy, J. Staš, H. Roubík, Renewable energy powered membrane desalination - review of recent development, Environ. Sci. Pollut. Res. Int. (2022), https://doi.org/10.1007/s11356-022-20480-y.
[20] N. Voutchkov, Energy use for membrane seawater desalination – current status and trends, Desalination 431 (2018) 2–14, https://doi.org/10.1016/j.desal.2017.10.033.
[21] Solargis, Weather data and software for solar power investments. https://solargis.com/maps-and-gis-data/download/world, 2023. (Accessed 21 May 2023).
[22] FAO, Food and Agriculture Organization of the United Nations. http://www.fao.org/sustainable-development-goals/indicators/642/en/, 2022 (accessed 21 May 2023).
[23] N. Ghaffour, I.M. Mujtaba, Desalination using renewable energy, Desalination 435 (2018) 1–2, https://doi.org/10.1016/j.desal.2018.01.029.
[24] O. Mahian, J. Wei, R.A. Taylor, S. Wongwises, Solar-driven Water Treatment: Re-engineering and Accelerating Nature's Water Cycle, Academic Press, 2022.
[25] V.N.X. Que, D. van Tuan, N.N. Huy, V. Le Phu, Design and performance of small-scale reverse osmosis desalination for brackish water powered by photovoltaic

units: a review, IOP Conf. Ser.: Earth Environ. Sci. 652 (2021) 12024, https://doi.org/10.1088/1755-1315/652/1/012024.
[26] L. Da Silva Lima, M. Quartier, A. Buchmayr, D. Sanjuan-Delmás, H. Laget, D. Corbisier, J. Mertens, J. Dewulf, Life cycle assessment of lithium-ion batteries and vanadium redox flow batteries-based renewable energy storage systems, Sustainable Energy Technol. Assess. 46 (2021) 101286, https://doi.org/10.1016/j.seta.2021.101286.
[27] International Renewable Energy Agency, Electricity Storage and Renewables: Costs and Markets to 2030, Abu Dhabi, 2017.
[28] C.-S. Karavas, K.G. Arvanitis, G. Kyriakarakos, D.D. Piromalis, G. Papadakis, A novel autonomous PV powered desalination system based on a DC microgrid concept incorporating short-term energy storage, Sol. Energy 159 (2018) 947–961, https://doi.org/10.1016/j.solener.2017.11.057.
[29] A. Sanna, B. Buchspies, M. Ernst, M. Kaltschmitt, Decentralized brackish water reverse osmosis desalination plant based on PV and pumped storage - technical analysis, Desalination 516 (2021), 115232, https://doi.org/10.1016/j.desal.2021.115232.
[30] A. Panagopoulos, K.-J. Haralambous, M. Loizidou, Desalination brine disposal methods and treatment technologies - a review, Sci. Total Environ. 693 (2019), 133545, https://doi.org/10.1016/j.scitotenv.2019.07.351.
[31] G. Cipolletta, N. Lancioni, Ç. Akyol, A.L. Eusebi, F. Fatone, Brine treatment technologies towards minimum/zero liquid discharge and resource recovery: state of the art and techno-economic assessment, J. Environ. Manag. 300 (2021), 113681, https://doi.org/10.1016/j.jenvman.2021.113681.
[32] MathWorks, MATLAB/Simulink, United States, 2018.
[33] S. Li, Y.-H. Cai, A.I. Schäfer, B.S. Richards, Renewable energy powered membrane technology: a review of the reliability of photovoltaic-powered membrane system components for brackish water desalination, Appl. Energy 253 (2019), 113524, https://doi.org/10.1016/j.apenergy.2019.113524.
[34] M.A. Khan, S. Rehman, F.A. Al-Sulaiman, A hybrid renewable energy system as a potential energy source for water desalination using reverse osmosis: a review, Renew. Sust. Energ. Rev. 97 (2018) 456–477, https://doi.org/10.1016/j.rser.2018.08.049.
[35] J.J. Roberts, A. Marotta Cassula, J.L. Silveira, E. Da Costa Bortoni, A. Z. Mendiburu, Robust multi-objective optimization of a renewable based hybrid power system, Appl. Energy 223 (2018) 52–68, https://doi.org/10.1016/j.apenergy.2018.04.032.
[36] J. Kim, S. Hong, A novel single-pass reverse osmosis configuration for high-purity water production and low energy consumption in seawater desalination, Desalination 429 (2018) 142–154, https://doi.org/10.1016/j.desal.2017.12.026.
[37] F. Alvarado-Revilla, H. Brown, M. Charamidi, I. Elkins (Eds.), Desalination Markets 2016, Oxford, United Kingdom, 2015.
[38] N. Voutchkov, Desalination Engineering: Planning and Design, McGraw-Hill, New York, 2013.
[39] G.D. Pimentel da Silva, M.H. Sharqawy, Techno-economic analysis of low impact solar brackish water desalination system in the Brazilian semiarid region, J. Clean. Prod. (2019), 119255, https://doi.org/10.1016/j.jclepro.2019.119255.
[40] Y. Du, L. Xie, Y. Liu, S. Zhang, Y. Xu, Optimization of reverse osmosis networks with split partial second pass design, Desalination 365 (2015) 365–380, https://doi.org/10.1016/j.desal.2015.03.019.
[41] M. Molinos-Senante, D. González, Evaluation of the economics of desalination by integrating greenhouse gas emission costs: an empirical application for Chile, Renew. Energy 133 (2019) 1327–1337, https://doi.org/10.1016/j.renene.2018.09.019.
[42] S.-Y. Pan, A.Z. Haddad, A. Kumar, S.-W. Wang, Brackish water desalination using reverse osmosis and capacitive deionization at the water-energy nexus, Water Res. 183 (2020), 116064, https://doi.org/10.1016/j.watres.2020.116064.
[43] N. Voutchkov, Desalination Project Cost Estimating and Management, CRC Press, Taylor & Francis Group, Boca Raton, London, New York, 2019.
[44] I.D. Spyrou, J.S. Anagnostopoulos, Design study of a stand-alone desalination system powered by renewable energy sources and a pumped storage unit, Desalination 257 (2010) 137–149, https://doi.org/10.1016/j.desal.2010.02.033.
[45] Rechnerphotovoltaik.de. https://www.rechnerphotovoltaik.de/photovoltaik/kosten-finanzierung/kosten-preise, 2022 (accessed 9 November 2022).
[46] B.A. Bhayo, H.H. Al-Kayiem, S.I. Gilani, Assessment of standalone solar PV-battery system for electricity generation and utilization of excess power for water pumping, Sol. Energy 194 (2019) 766–776, https://doi.org/10.1016/j.solener.2019.11.026.
[47] C. Brown, R. Poudineh, B. Foley, Achieving a Cost-Competitive Offshore Wind Power Industry: What Is the Most Effective Policy Framework? Oxford Institute for Energy Studies, Oxford, 2015.
[48] B. Wu, A. Maleki, F. Pourfayaz, M.A. Rosen, Optimal design of stand-alone reverse osmosis desalination driven by a photovoltaic and diesel generator hybrid system, Sol. Energy 163 (2018) 91–103, https://doi.org/10.1016/j.solener.2018.01.016.
[49] K. Bognar, P. Blechinger, F. Behrendt, Seawater desalination in micro grids: an integrated planning approach, Energy Sustain. Soc. 2 (2012), https://doi.org/10.1186/2192-0567-2-14.
[50] Ministry of Environment, Updated Submission of Jordan's 1st Nationally Determined Contribution (NDC), Amman, Jordan, 2021.
[51] International Renewable Energy Agency, Renewables Readiness Assessment: The Hashemite Kingdom of Jordan, Abu Dhabi, 2021.
[52] L.M. Halabi, S. Mekhilef, L. Olatomiwa, J. Hazelton, Performance analysis of hybrid PV/diesel/battery system using HOMER: a case study Sabah, Malaysia, Energy Convers. Manag. 144 (2017) 322–339, https://doi.org/10.1016/j.enconman.2017.04.070.
[53] M.O. Atallah, M.A. Farahat, M.E. Lotfy, T. Senjyu, Operation of conventional and unconventional energy sources to drive a reverse osmosis desalination plant in Sinai Peninsula, Egypt, Renew. Energy 145 (2020) 141–152, https://doi.org/10.1016/j.renene.2019.05.138.
[54] M.M. Ibrahim, N.H. Mostafa, A.H. Osman, A. Hesham, Performance analysis of a stand-alone hybrid energy system for desalination unit in Egypt, Energy Convers. Manag. 215 (2020), 112941, https://doi.org/10.1016/j.enconman.2020.112941.
[55] Y. Jiang, J. Zhao, Z. Tong, Optimum design of a solar-wind-diesel hybrid energy system with multiple types of storage devices driving a reverse osmosis desalination process, Processes 10 (2022) 2199, https://doi.org/10.3390/pr10112199.
[56] M.S. Ismail, M. Moghavvemi, T. Mahlia, Techno-economic analysis of an optimized photovoltaic and diesel generator hybrid power system for remote houses in a tropical climate, Energy Convers. Manag. 69 (2013) 163–173, https://doi.org/10.1016/j.enconman.2013.02.005.
[57] A. Setas Lopes, R. Castro, C.S. Silva, Design of water pumped storage systems: a sensitivity and scenario analysis for island microgrids, Sustainable Energy Technol. Assess. 42 (2020), 100847, https://doi.org/10.1016/j.seta.2020.100847.
[58] Y.F. Nassar, M.J. Abdunnabi, M.N. Sbeta, A.A. Hafez, K.A. Amer, A.Y. Ahmed, B. Belgasim, Dynamic analysis and sizing optimization of a pumped hydroelectric storage-integrated hybrid PV/wind system: a case study, Energy Convers. Manag. 229 (2021), 113744, https://doi.org/10.1016/j.enconman.2020.113744.
[59] M. Shabani, E. Dahlquist, F. Wallin, J. Yan, Techno-economic comparison of optimal design of renewable-battery storage and renewable micro pumped hydro storage power supply systems: a case study in Sweden, Appl. Energy 279 (2020), 115830, https://doi.org/10.1016/j.apenergy.2020.115830.
[60] International Renewable Energy Agency, Renewable Power Generation Costs in 2017, Abu Dhabi, 2018.
[61] International Renewable Energy Agency, Renewable Power Generation Costs in 2018, Abu Dhabi, 2019.
[62] M. Guezgouz, J. Jurasz, B. Bekkouche, T. Ma, M.S. Javed, A. Kies, Optimal hybrid pumped hydro-battery storage scheme for off-grid renewable energy systems, Energy Convers. Manag. 199 (2019), 112046, https://doi.org/10.1016/j.enconman.2019.112046.
[63] Q. Khan, M.A. Maraqa, A.-M.O. Mohamed, Inland desalination, in: Pollution Assessment for Sustainable Practices in Applied Sciences and Engineering, Elsevier, 2021, pp. 871–918.
[64] K. Elsaid, M. Kamil, E.T. Sayed, M.A. Abdelkareem, T. Wilberforce, A. Olabi, Environmental impact of desalination technologies: a review, Sci. Total Environ. 748 (2020), 141528, https://doi.org/10.1016/j.scitotenv.2020.141528.
[65] K. Elsaid, E.T. Sayed, M.A. Abdelkareem, M.S. Mahmoud, M. Ramadan, A. G. Olabi, Environmental impact of emerging desalination technologies: a preliminary evaluation, J. Environ. Chem. Eng. 8 (2020), 104099, https://doi.org/10.1016/j.jece.2020.104099.
[66] I. Ihsanullah, M.A. Atieh, M. Sajid, M.K. Nazal, Desalination and environment: a critical analysis of impacts, mitigation strategies, and greener desalination technologies, Sci. Total Environ. 780 (2021), 146585, https://doi.org/10.1016/j.scitotenv.2021.146585.
[67] A. Giwa, V. Dufour, F. Al Marzooqi, M. Al Kaabi, S.W. Hasan, Brine management methods: recent innovations and current status, Desalination 407 (2017) 1–23, https://doi.org/10.1016/j.desal.2016.12.008.
[68] M. Khan, M.A. Al-Ghouti, DPSIR framework and sustainable approaches of brine management from seawater desalination plants in Qatar, J. Clean. Prod. 319 (2021), 128485, https://doi.org/10.1016/j.jclepro.2021.128485.
[69] S. Timmerberg, A. Sanna, M. Kaltschmitt, M. Finkbeiner, Renewable electricity targets in selected MENA countries – assessment of available resources, generation costs and GHG emissions, Energy Rep. 5 (2019) 1470–1487, https://doi.org/10.1016/j.egyr.2019.10.003.
[70] E. Santoyo-Castelazo, K. Solano-Olivares, E. Martínez, E.O. García, E. Santoyo, Life cycle assessment for a grid-connected multi-crystalline silicon photovoltaic system of 3 kWp: a case study for Mexico, J. Clean. Prod. 316 (2021), 128314, https://doi.org/10.1016/j.jclepro.2021.128314.
[71] International Sustainability & Carbon Certification, ISCC EU 205 Greenhouse Gas Emissions. https://www.iscc-system.org/process/iscc-documents-at-a-glance/iscc-system-documents/ (accessed 21 May 2023).
[72] H.M.K. Al-Masri, S.K. Magableh, A. Abuelrub, O. Saadeh, M. Ehsani, Impact of different photovoltaic models on the design of a combined solar array and pumped hydro storage system, Appl. Sci. 10 (2020) 3650, https://doi.org/10.3390/app10103650.
[73] Guidelines for Estimating Greenhouse Gas Emissions of ADB Projects, Asian Development Bank, Manila, Philippines, 2017.
[74] S. Baurzhan, G. Jenkins, On-grid solar PV versus diesel electricity generation in sub-Saharan Africa: economics and GHG emissions, Sustainability 9 (2017) 372, https://doi.org/10.3390/su9030372.
[75] M.A. Ashraf, Z. Liu, A. Alizadeh, S. Nojavan, K. Jermsittiparsert, D. Zhang, Designing an optimized configuration for a hybrid PV/diesel/battery energy system based on metaheuristics: a case study on Gobi Desert, J. Clean. Prod. 270 (2020), 122467, https://doi.org/10.1016/j.jclepro.2020.122467.
[76] M.S. Javed, T. Ma, J. Jurasz, J. Mikulik, A hybrid method for scenario-based techno-economic-environmental analysis of off-grid renewable energy systems, Renew. Sust. Energ. Rev. 139 (2021), 110725, https://doi.org/10.1016/j.rser.2021.110725.
[77] G. Zubi, R. Dufo-López, N. Pardo, G. Pasaoglu, Concept development and techno-economic assessment for a solar home system using lithium-ion battery for developing regions to provide electricity for lighting and electronic devices,

Energy Convers. Manag. 122 (2016) 439–448, https://doi.org/10.1016/j.enconman.2016.05.075.
[78] S. Jenu, I. Deviatkin, A. Hentunen, M. Myllysilta, S. Viik, M. Pihlatie, Reducing the climate change impacts of lithium-ion batteries by their cautious management through integration of stress factors and life cycle assessment, J. Energy Storage 27 (2020), 101023, https://doi.org/10.1016/j.est.2019.101023.
[79] J.F. Peters, M. Baumann, B. Zimmermann, J. Braun, M. Weil, The environmental impact of Li-ion batteries and the role of key parameters – a review, Renew. Sust. Energ. Rev. 67 (2017) 491–506, https://doi.org/10.1016/j.rser.2016.08.039.
[80] PVGIS 5.2, Photovoltaic Geographical Information System. http://re.jrc.ec.europa.eu/pvgis.html, 2019. (Accessed 2 March 2022).
[81] D.S. Ayou, H.M. Ega, A. Coronas, A feasibility study of a small-scale photovoltaic-powered reverse osmosis desalination plant for potable water and salt production in Madura Island: a techno-economic evaluation, Therm. Sci. Eng. Prog. 35 (2022), 101450, https://doi.org/10.1016/j.tsep.2022.101450.
[82] Trading economics, Jordan Interest Rate. https://tradingeconomics.com/jordan/interest-rate, 2023. (Accessed 19 May 2023).
[83] Y. Elsaie, H. Soussa, M. Gado, A. Balah, Water desalination in Egypt; literature review and assessment, Ain Shams Eng. J. (2022), 101998, https://doi.org/10.1016/j.asej.2022.101998.
[84] V.J. Subiela-Ortín, B. Peñate-Suárez, J.A. de La Fuente-Bencomo, Main technical and economic guidelines to implement wind/solar-powered reverse-osmosis desalination systems, Processes 10 (2022) 653, https://doi.org/10.3390/pr10040653.
[85] Big Brand Water Filter Inc, Brackish Water Membranes: Dow Filmtec BW30HR LE-440i. https://www.bigbrandwater.com/search.asp?keyword=Dow+Filmtec+BW30HR+LE-440i, 2022 (accessed 9 November 2022).
[86] F. Ameen, J.A. Stagner, D.S.-K. Ting, The carbon footprint and environmental impact assessment of desalination, Int. J. Environ. Stud. 75 (2018) 45–58, https://doi.org/10.1080/00207233.2017.1389567.
[87] T.N. Bitaw, K. Park, J. Kim, J.W. Chang, D.R. Yang, Low-recovery, -energy-consumption, -emission hybrid systems of seawater desalination: energy optimization and cost analysis, Desalination 468 (2019), 114085, https://doi.org/10.1016/j.desal.2019.114085.
[88] J. Liu, S. Chen, H. Wang, X. Chen, Calculation of carbon footprints for water diversion and desalination projects, Energy Procedia 75 (2015) 2483–2494, https://doi.org/10.1016/j.egypro.2015.07.239.
[89] M. Heihsel, M. Lenzen, A. Malik, A. Geschke, The carbon footprint of desalination, Desalination 454 (2019) 71–81, https://doi.org/10.1016/j.desal.2018.12.008.
[90] National Multidisciplinary Team Jordan, Assessment of Food Supply under Water Scarcity Conditions in the Near East and North Africa Region: Applying the Food Supply Cost Curve Approach - Jordan Case Study. http://www.fao.org/3/ca1156en/CA1156EN.pdf, 2018 (accessed 4 September 2022).
[91] Royal HaskoningDHV and MASAR Center Jordan, National Master Plan for the Jordan River Valley. https://old.ecopeaceme.org/wp-content/uploads/2020/10/Jordanian_National_Master_Plan-2019_05_06-06_06_03-UTC.pdf (accessed 10 November 2022).
[92] E. Salameh, The tragedy of the Karama Dam Project/Jordan, Acta Hydrochim. Hydrobiol. 32 (2004) 249–258, https://doi.org/10.1002/aheh.200300533.
[93] N. Voutchkov, The Role of Desalination in an Increasingly Water-Scarce World, 2019, https://doi.org/10.1596/31416.
[94] I.E. Kosmadakis, C. Elmasides, G. Koulinas, K.P. Tsagarakis, Energy unit cost assessment of six photovoltaic-battery configurations, Renew. Energy (2021), https://doi.org/10.1016/j.renene.2021.03.010.
[95] A. Maleki, M.G. Khajeh, M.A. Rosen, Weather forecasting for optimization of a hybrid solar-wind–powered reverse osmosis water desalination system using a novel optimizer approach, Energy 114 (2016) 1120–1134, https://doi.org/10.1016/j.energy.2016.06.134.
[96] International Renewable Energy Agency, Renewable Technology Innovation Indicators: Mapping Progress in Costs, Patents and Standards, Abu Dhabi, 2022.
[97] solaranlagen-portal, Kosten einer Photovoltaikanlage in 2022. https://www.solaranlagen-portal.de/photovoltaik/preis-solar-kosten.html, 2022 (accessed 9 November 2022).
[98] National Renewable Energy Laboratory, Annual Technology Baseline. https://atb.nrel.gov/electricity/2022/utility-scale_pv, 2022 (accessed 9 November 2022).
[99] R. Bakhshi-Jafarabadi, J. Sadeh, M. Dehghan, Economic evaluation of commercial grid-connected photovoltaic systems in the Middle East based on experimental data: a case study in Iran, Sustainable Energy Technologies and Assessments 37 (2020), 100581, https://doi.org/10.1016/j.seta.2019.100581.
[100] National Renewable Energy Laboratory, Energy Analysis: Life Cycle Assessment Harmonization. https://www.nrel.gov/analysis/life-cycle-assessment.html, 2022. (Accessed 10 November 2022).
[101] R. Almasri, R. Sarkar, Decentralized Solar in Jordan: Financing the Future, Friedrich-Ebert-Stiftung Jordan et Iraq, Amman, 2021.
[102] G. Vinter, M. Norman, Jordan – Back to the future, Project Finance International. https://www.cov.com/-/media/files/corporate/publications/2019/03/jordan_back_to_the_future.pdf, 2019 (accessed 11 November 2022).
[103] Energy and Minerals Regulatory Commission, Electricity Tariff: Retail Supply Tariff. https://www.nepco.com.jo/en/default.aspx (accessed 19 May 2023).
[104] A. Albatayneh, A. Juaidi, R. Abdallah, A. Peña-Fernández, F. Manzano-Agugliaro, Effect of the subsidised electrical energy tariff on the residential energy consumption in Jordan, Energy Rep. 8 (2022) 893–903, https://doi.org/10.1016/j.egyr.2021.12.019.
[105] National Electric Power Company, Annual Report. https://www.nepco.com.jo/en/annual_report_en.aspx, 2019. (Accessed 8 November 2022).
[106] S. Kiwan, E. Al-Gharibeh, Jordan toward a 100% renewable electricity system, Renew. Energy 147 (2020) 423–436, https://doi.org/10.1016/j.renene.2019.09.004.
[107] NEPCO, National Electric Power Company: Annual Report 2020. https://www.nepco.com.jo/en/annual_report_en.aspx, 2020 (accessed 4 September 2022).
[108] S.S. Alrwashdeh, Energy sources assessment in Jordan, Res. Eng. Des. 13 (2022), 100329, https://doi.org/10.1016/j.rineng.2021.100329.
[109] M.R. Quitoras, P.E. Campana, C. Crawford, Exploring electricity generation alternatives for Canadian Arctic communities using a multi-objective genetic algorithm approach, Energy Convers. Manag. 210 (2020), 112471, https://doi.org/10.1016/j.enconman.2020.112471.
[110] W. Zhang, A. Maleki, Modeling and optimization of a stand-alone desalination plant powered by solar/wind energies based on back-up systems using a hybrid algorithm, Energy 254 (2022), 124341, https://doi.org/10.1016/j.energy.2022.124341.
[111] GlobalPetrolPrices.com, Retail energy price data: Jordan diesel prices. https://www.globalpetrolprices.com/Jordan/diesel_prices/, 2023 (accessed 26 April 2023).
[112] K. Elsaid, E.T. Sayed, M.A. Abdelkareem, A. Baroutaji, A.G. Olabi, Environmental impact of desalination processes: mitigation and control strategies, Sci. Total Environ. 740 (2020), 140125, https://doi.org/10.1016/j.scitotenv.2020.140125.
[113] United States Environmental Protection Agency, Greenhouse Gases Equivalencies Calculator - Calculations and References. https://www.epa.gov/energy/greenhouse-gases-equivalencies-calculator-calculations-and-references, 2023. (Accessed 21 September 2023).
[114] LiquiPipe, PE Rohr Trinkwasserrohr 12,5PN. https://www.liquipipe.de/p/pe-rohr-110mm-100m-0706088-100.html, 2022. (Accessed 10 November 2022).
[115] A. Gajic, V. Stevanovic, S. Pejovic, B. Karney, Hydro storage reduces electricity costs and keep wind and solar unpolluted, IOP Conf. Ser.: Earth Environ. Sci. 240 (2019) 82015, https://doi.org/10.1088/1755-1315/240/8/082015.
[116] P. Das, B.K. Das, N.N. Mustafi, M.T. Sakir, A review on pump-hydro storage for renewable and hybrid energy systems applications, Energy Storage 3 (2021), https://doi.org/10.1002/est2.223.
[117] Z. Guo, S. Ge, X. Yao, H. Li, X. Li, Life cycle sustainability assessment of pumped hydro energy storage, Int. J. Energy Res. 44 (2020) 192–204, https://doi.org/10.1002/er.4890.
[118] mg-solar, LG CHEM RESU 10 Lithium Ionen Speicher Akku. https://www.mg-solar-shop.de/Batteriespeichersysteme/LG-CHEM-RESU-10-Lithium-Ionen-10-kWh-Speicher-Akku.html, 2022. (Accessed 10 November 2022).
[119] mg-solar, SolarEdge SE5000H HD-WAVE SetApp STOREDGE. https://www.mg-solar-shop.de/SolarEdge-SE5000H-HD-WAVE-SetApp-STOREDGE, 2022 (accessed 10 November 2022).
[120] F.A.M. de Faria, P. Jaramillo, H.O. Sawakuchi, J.E. Richey, N. Barros, Estimating greenhouse gas emissions from future Amazonian hydroelectric reservoirs, Environ. Res. Lett. 10 (2015), 124019, https://doi.org/10.1088/1748-9326/10/12/124019.
[121] M.A. Jones, I. Odeh, M. Haddad, A.H. Mohammad, J.C. Quinn, Economic analysis of photovoltaic (PV) powered water pumping and desalination without energy storage for agriculture, Desalination 387 (2016) 35–45, https://doi.org/10.1016/j.desal.2016.02.035.